SANDIA REPORT

SAND92–2253 • UC–233
Unlimited Release
Printed June 1993

Bench-Scale Screening Tests for a Boiling Sodium-Potassium Alloy Solar Receiver

J. B. Moreno, T. A. Moss

Prepared by
Sandia National Laboratories
Albuquerque, New Mexico 87185 and Livermore, California 94550
for the United States Department of Energy
under Contract DE-AC04-76DP00789

SF2900Q(8-81)

Issued by Sandia National Laboratories, operated for the United States Department of Energy by Sandia Corporation.

Printed in the United States of America. This report has been reproduced directly from the best available copy.

Available to DOE and DOE contractors from
Office of Scientific and Technical Information
PO Box 62
Oak Ridge, TN 37831

Prices available from (615) 576-8401, FTS 626-8401

Available to the public from
National Technical Information Service
US Department of Commerce
5285 Port Royal Rd
Springfield, VA 22161

NTIS price codes
Printed copy: A04
Microfiche copy: A01

SAND92-2253
Unlimited Release
Printed June 1993

Distribution
Category UC-233

Bench-Scale Screening Tests for a Boiling Sodium-Potassium Alloy Solar Receiver

J. B. Moreno
T. A. Moss
Solar Thermal Technology Department

Sandia National Laboratories
Albuquerque, New Mexico 87185

Abstract

Bench-scale tests were carried out in support of the design of a second-generation 75-kW_t reflux pool-boiler solar receiver. The receiver will be made from Haynes Alloy 230 and will contain the sodium-potassium alloy NaK-78. The bench-scale tests used quartz-lamp-heated boilers to screen candidate boiling-stabilization materials and methods at temperatures up to 750°C. Candidates that provided stable boiling were tested for hot-restart behavior. Poor stability was obtained with single 1/4-inch diameter patches of powdered metal hot-press-sintered onto the wetted side of the heat-input area. Laser-drilled and electric-discharge-machined cavities in the heated surface also performed poorly. Small additions of xenon, and heated-surface tilt out of the vertical dramatically improved poor boiling stability; additions of helium or oxygen did not. The most stable boiling was obtained when the entire heat-input area was covered by a powdered-metal coating. The effect of heated-area size was assessed for one coating: at low incident fluxes, when even this coating performed poorly, increasing the heated-area size markedly improved boiling stability. Good hot-restart behavior was not observed with any candidate, although results were significantly better with added xenon in a boiler shortened from 3 to 2 feet. In addition to the screening tests, flash-radiography imaging of metal-vapor bubbles during boiling was attempted. Contrary to the Cole-Rohsenow correlation, our bubble-size estimates did not vary with pressure; instead they were constant, consistent with the only other alkali metal measurements, but about 1/2 their size.

Acknowledgments

The authors are indebted to Chuck Andraka and Rich Diver for valuable discussions, Scott Rawlinson for support coordination at Sandia's National Solar Thermal Test Facility, Vern Dudley for data and control computer programming, Daniel Ray for on-site fabrication of test fixtures, John Murray for flash radiography, Phil Baca for image digitization, and Craig Ginn for image enhancement assistance.

Contents

Figures

1 Introduction

Refluxing liquid-metal solar receivers are being developed to serve as the interface between dish concentrators and Stirling engines. This effort is underway at private and government laboratories here and abroad [1,2,3]. At Sandia National Laboratories, reflux receiver development is funded by the United States Department of Energy's Solar Thermal Technology Program.

Two types of reflux receivers are being developed: pool boilers and heat pipes. Figure 1 illustrates the pool-boiler concept. A pool of liquid alkali-metal is heated by solar flux concentrated on an absorber surface. The liquid boils, cooling the absorber. The vapor flows to the Stirling-engine heater tubes, where it condenses, providing heat to run the engine. The liquid condensate flows back to the pool, completing the heat-transport cycle. In contrast to the pool-boiler receiver, the heat-pipe uses a wick instead of the pool to ensure that the absorber is covered with liquid-metal coolant. In the anticipated operating-temperature range, 700 to 800°C, the alkali metals sodium and potassium have vapor pressures conveniently near one atmosphere, which is high enough for efficient heat transfer yet is structurally undemanding.

The liquid-metal reflux receiver concept is an attractive alternative to directly-illuminated engine heater tubes, because it provides an essentially isothermal heat input over the surface of the engine heater-head tubes. This results in improved engine lifetime and efficiency. It also decouples the design of the absorber from the design of the heater tubes, allowing separate optimizations. In the case of hybrid designs, the reflux receiver also decouples the design of the afore-mentioned surfaces from the design of the gas-fired surface.

The pool-boiler and heat-pipe concepts each have advantages and disadvantages. The pool-boiler receiver has few parts and is simple to construct, but some design tools are not yet mature, and it requires a considerable liquid-metal inventory -- 13 pounds of sodium in the first 75-kW_t demonstration. The design tools that require further development are associated with three boiling-behavior concerns: boiling instability, the hot-restart problem and the heat-transfer crises of film boiling and flooding. All three boiling-behavior concerns are discussed in greater detail in Section 2.3. Boiling instability is the random switching between boiling and natural convection, common in liquid metals. The hot-restart problem refers to the high temperatures often required to resume momentarily-interrupted boiling. Film boiling and flooding are failures of liquid to return to the heated surface on local and global scales respectively. In contrast to the pool-boiler, the heat-pipe receiver has a more well-developed set of design tools and a small liquid-metal inventory --

6 pounds of sodium in the first 75-kW_t prototype. However, at the 75-kW_t level the heat-pipe receiver requires a complex wick/artery structure for which the design tools are not yet proven [4].

The first pool-boiler reflux receiver, shown in Figure 2, was operated at Sandia National Laboratories in the Fall of 1989 and Spring of 1990, at up to 62 kW_t throughput power and 800°C vapor temperature [5,6,7]. From extensive evidence in the literature and from our own bench-scale tests, we expected that boiling would not be stable without special control techniques [8,9,10]. Boiling requires the presence of nucleation sites (gas or vapor-filled voids) from which vapor bubbles can grow. These voids are usually natural microscopic cavities in the heated surface. The LaPlace bubble equilibrium equation shows that the smaller the nucleation site the higher the wall superheat required to initiate bubble growth [8]. In unstable boiling it appears that the larger natural cavities present in a heated surface become "deactivated" -- filled with liquid metal -- and steady boiling stops. The wall superheat increases in order to drive the less-efficient natural-convection heat transfer mode. The superheat may increase enough to explosively inflate a bubble at one of the smaller nucleation sites. This often seems to be followed by reactivation of one or more larger sites and steady boiling resumes. To achieve stable boiling, our first boiler was built with 35 equally-spaced "artificial cavities" 0.006" in diameter by 0.02" deep electric-discharge-machined (EDM) in the wetted side of the absorber. According to the boiling-stability theory of Shai and Rohsenow, these cavities were deep enough to avoid deactivation[8]. Passive control of the hot-restart problem was achieved by adding a trace of xenon to the boiler headspace, as suggested by Saaski [11].

During the testing of the first pool-boiler receiver, two important boiling-behavior concerns were at least partially settled: excellent boiling stability was demonstrated under all conditions, and good hot-restart behavior was demonstrated at sun elevations up to about 60 degrees. After approximately 50 hours of testing, the receiver developed a leak during an unusually low-temperature restart in late May, 1990. Post-test analysis indicated that the leak was most probably a result of heat-transfer crisis (film boiling or flooding) as a result of the unusual restart conditions [7]. This conclusion was based on comparisons of the actual heat fluxes with estimates of the critical heat fluxes for each type of crisis.

Since the first pool-boiler receiver demonstration, the reflux receiver program at Sandia has emphasized moving the pool-boiler receiver concept closer to commercialization. The strategy has been to (1) determine what changes will improve commercial potential, (2) identify candidate materials and methods to achieve those changes, (3) screen the candidate materials and methods in short-term bench-scale tests, (4) design, build and demonstrate a 2nd-generation pool-boiler receiver based on the outcome of the short-term tests, and (5) demonstrate lifetime potential in long-term bench-scale tests. The present report recaps the outcome of items 1 and 2, and presents in detail the results of item 3 -- the short-term bench-scale screening tests.

2 Materials and Methods for Improved Commercial Potential

We have determined three major changes that will improve the commercial potential of the pool-boiler receiver: (1) reducing the cost, (2) increasing robustness and lifetime, and (3) improving the design tools. In the following subsections these changes and the materials and methods identified to effect them are discussed.

2.1 Reducing Cost

Two potential cost reductions were identified. The first is the elimination of the electrical preheaters used to melt the sodium in the receiver. Because sodium expands on melting, preheating must be done with care before going on sun, to avoid damage to the receiver. The preheaters, shown in Figure 3, cost approximately $360. In addition to this initial expense, replacement costs over the lifetime of the receiver are expected. Other problems associated with preheating include the time required to melt the sodium, as illustrated in Figure 4, and the cost of the electricity itself. For many geographical locations, the preheaters can be eliminated by replacing the sodium in the receiver with NaK-78, which freezes at -12.6 ^{o}C. The extra cost of the NaK-78 -- less than $123 for 20 pounds [12] -- is clearly justified.

The second potential cost reduction is the elimination of the 35 electric-discharge-machined (EDM) cavities. A cross-section of an EDM cavity from the first pool boiler receiver is shown in Figure 5. As mentioned earlier, the heated surface was modified by the installation of these cavities to ensure stable boiling, with the cavity dimensions chosen in accordance with the stability theory of Shai and Rohsenow [8]. The expense of machining these cavities was $100 each, or $3500 total. The high cost is a function of the slow speed of the EDM process and the cost of the machine. A less-expensive alternative is pulsed-laser drilling. At Sandia, a technique has been developed to drill cavities roughly equivalent to the EDM cavities, using a pulsed YAG laser [13]. Because drilling each hole takes only as long as the time to position the workpiece, we have estimated a cost for 35 cavities of only about $14 including labor and overhead [12]. One objection to cavities is that they cause stress concentrations in the absorber. Even when the design allows for these stress concentrations, the perception of a problem may remain and adversely impact commercialization.

Another economical method to stabilize boiling that avoids the stress-concentration problem of cavities has been demonstrated by Thermacore, Inc. [14]. They used a hot-press-sintered powder-metal coating made from -100+140 mesh 304L stainless-steel powder with a boiler tube made from Inconel 625. How this coating stabilizes boiling is currently a matter of speculation. In adapting the concept to Sandia's pool-boiler development program, it was desired to match the thermal-expansion characteristics of the coating material to those of the boiler wall, within the constraint of powder availability. This reduces the thermal stresses at the coating/wall interface, and in turn can lower the requirements on interfacial strength and the prospect of fatigue failure at the interface. The candidate material that was chosen was Inconel 600. Type 304L stainless steel was a second choice, selected in order to verify the Thermacore results. In order to develop adequate interfacial strength, it was found necessary to press the powder metals against the boiler wall during the high-temperature sintering run. For a spherical-segment absorber such as is used in current pool-boiler receiver designs, hot pressing introduces very difficult fixturing problems. These problems are lessened if the coating is only required as discrete patches. If a discrete patch provides at least one stable nucleation site, analogous to an EDM cavity, then an array of equally-spaced patches should ensure stable boiling in a pool-boiler receiver. Discrete powder-metal patches was one of several candidate powder-metal-coating stabilization methods selected for screening.

An alternative powder-metal coating scheme that avoids the requirement of hot pressing is brazed powders. In this approach, the coating powder is mixed with a braze alloy powder which fuses to join the coating particles to themselves and to the boiler wall. Because pressing is not required, continuous coatings over an entire absorber dome may be relatively simple to achieve. A number of coating samples were supplied to Sandia by Friction Coatings, Inc. for screening. We have estimated the cost of a powder metal coating at \$127 for production rates of 10^4/year [12].

A final possibility to be considered is that noncondensible gases such as xenon, added to the pool-boiler vapor space, might stabilize boiling. We have postulated that boiling will cause liquid metal to be thrown above the pool surface where it may entrain and carry into the pool small bubbles of gas, and that some of these bubbles may come close enough to the heated surface to serve as nucleation sites. This mechanism and an alternative are discussed in Section 2.3.2. Our estimate for the cost of adding gas is \$18 [15].

2.2 Increasing Robustness and Lifetime

Robustness and lifetime are related issues. Here robustness refers to the factors of safety for mechanical strength and heat transfer. Lifetime refers to the factors of safety for creep, fatigue and corrosion failures, as well as to the long-term prospect for stable liquid-metal boiling. The measures planned to improve robustness and lifetime in the 2nd-generation pool-boiler receiver have been detailed in previous reports [6,7]: (1) replace 316L stainless steel by Haynes Alloy 230; (2) increase the size (radius of curvature and rim diameter) of the absorber, (3) increase the gap between the absorber and the rear dome; and (4) decrease the thickness of the rear dome. These changes are based on heat-transfer and stress analyses, and on recommendations made by a panel of materials specialists at Sandia.

The increase in absorber size and dome gap will improve the factor of safety against heat-transfer crises, and will be proven in the full-scale test of the 2nd-generation receiver. The decrease in rear-dome thickness will reduce stresses near the edge of the absorber, by presenting a less rigid constraint. The material choice, Haynes Alloy 230, will provide greater strength and thermal stability, and much-lower air-side and flue-gas corrosion rates. However, the long-term effect of boiling NaK-78 on Haynes Alloy 230 is not known. This is one reason that bench-scale lifetime tests are necessary.

2.3 Improving Design Tools

The information necessary for the design of a liquid-metal pool-boiler receiver includes (1) the flux distribution produced by the concentrator, (2) the heat loss and net-flux distribution on the absorber, (3) temperature distributions -- most importantly over the absorber surface and through its thickness, (4) stress distributions -- again most importantly for the absorber, and (5) criteria for the avoidance of boiling instability, hot-restart failure and heat-transfer crisis. The tools necessary to predict distributions of gross and net solar flux, temperature, and stress (items 1-4), are well developed [16,17,18]. The state of knowledge is much less satisfactory when it comes to the liquid-metal boiling-behavior issues listed in item 5. Dwyer has pointed out in his book the large number of independent variables that govern some aspects of boiling behavior, and the consequent conflicting results reported from different laboratories [19]. In the current bench-scale tests, the emphasis has been on screening stabilization methods for use in a Haynes Alloy 230 boiler containing NaK-78. Nevertheless, we have tried to improve our understanding of liquid-metal boiling behavior by including issue-specific tests as resources allowed. An outline of liquid-metal boiling-behavior issues follows.

2.3.1 Boiling Stability

The tendency of alkali metals to boil unstably as reviewed in the Introduction is well known [20]. Unstable boiling can be described as random cycling between boiling and non-boiling. When boiling stops, the heated-surface temperature increases in order to drive the remaining less-efficient heat-transfer modes -- mainly natural convection. The cessation and restart of boiling, and particularly the processes of nucleation site deactivation and reactivation are poorly understood.

The most extensive work in this area has been by Rohsenow and his students at the Massachusetts Institute of Technology [21]. They showed that stable boiling can be achieved by suitable modification of the wetted side of the heated surface. Shai and Rohsenow derived a simple stability condition for slender cylindrical cavities [8]:

$$q_{min} \propto \left[h + \frac{\sqrt{k_l \rho_l \alpha_l}}{\ell} \Im\left(\sqrt{\frac{k_w \rho_w c_w}{k_l \rho_l c_l}} \right) \right] \frac{T_{sat}^2 \sigma}{r P_{sat}} , \tag{1}$$

Here q_{min} is the minimum heat flux for stability, h is a convective heat-transfer coefficient, ℓ is the cavity depth, r is the cavity radius, T_{sat} and P_{sat} are the vapor temperature and pressure, σ is the surface tension, and $\Im$ is a function of k, ρ and c -- respectively the heat conductivity, density and heat capacity -- of the heated wall when the subscript is w, and of the liquid metal when the subscript is l. This expression indicates that for a given boiler, stability improves with increasing heat flux or temperature (since T_{sat}^2/P_{sat} decreases as T_{sat} increases). Shai and Rohsenow assumed a value for h to force this expression to fit their results, but in general h is unknown. The derivation of Equation 1 assumes thermal equilibrium between the cavity wall and the liquid entering the cavity, but neglects inertial and viscous effects. Shai and Rohsenow were able to show that the trends predicted by their stability condition are consistent with the few data available. Nevertheless, in the paper's discussion section they agree with a comment that the consistency may be accidental.

The point of this brief review is that there are no reliable tools for the design of a <u>stable</u> alkali-metal boiler. Moreover, there is so little experience with stable boiling of alkali metals that there aren't even accepted rules of thumb for design. Among the many questions that can be posed are:

1. What guarantees stability of a nucleation site?
2. In a given boiler, how many stable nucleation sites are necessary?
3. Can stable boiling be achieved without stable nucleation sites, i.e., can a critical density of unstable sites guarantee stability?

4. What is the effect of heated-surface orientation on stability?

5. What is the effect of heated-surface size?

6. What is the effect of added non-condensible gas?

7. Will there always be active nucleation sites available for startup? What is their nature?

8. Why won't all the sites that initiate boiling eventually be filled with liquid metal?

9. The large wall superheats typically seen during startup suggest that only small nucleation sites are initially active. The small superheats seen during sustained stable boiling suggest that large nucleation sites have been activated. How do the large sites get activated?

2.3.2 Hot Restart Behavior

The "hot restart problem" has been described in previous reports on both bench-scale and full-scale sodium boilers and a bench-scale NaK boiler [5,10,22]. The problem arises when the heat input is briefly but repeatedly interrupted, as during cloud transients. In the full-scale test, typically on the third cycle, boiling would not resume until a very large wall superheat -- greater than 100^{o}C -- had been reached. Often these superheats are greater than those seen in cold starts, for reasons unknown. Here superheat is defined as the temperature difference between the wall and the vapor above the pool. In many cases during the full-scale hot-restart tests, high-temperature protection systems interrupted the heat source before boiling began.

The hot-restart problem has been passively controlled under some conditions [5,7,14] by adding a noncondensible gas to the boiler headspace as suggested by Saaski [11]. In the only on-sun test of this method, good hot-restart behavior was obtained for sun elevations less than about 60 degrees. We have taken this as evidence that the method works by entrainment of the gas into the liquid-metal pool. This process is as follows: the gas is swept and compressed into the rear of the condenser by the flow of metal vapor from the pool to the condenser. A film of liquid metal coats the condenser surfaces. Entrainment occurs when metal droplets are flung from the pool through the compressed gas and into the liquid film by the boiling action. During a hot restart, gas bubbles adjacent to the heated surface serve as nucleation sites . As operation of the receiver is extended to higher sun elevations, the metal droplets must be thrown a greater vertical distance above the pool to reach the compressed gas. Eventually they can no longer reach the gas cap, and the method fails. If this hypothesis is correct, the method will be dependent on configuration as well as orientation. It will also be sensitive to the density of the gas relative to the vapor, since that affects whether or not the position of the compressed gas, above the vapor, is stable.

An alternative explanation for the effect of added gas on hot-restart behavior is that the gas dissolves in the liquid metal during periods of steady boiling, and precipitates out when heating is interrupted and the receiver cools [14]. If correct, this explanation would suggest choosing a gas based on solubility rather than entrainment considerations.

The hot-restart problem has also been controlled by an active method which we call "load control" [5,23]. In this method, the thermal load that cools the condenser is deliberately maximized when the heat input to the receiver is interrupted. This lowers the metal-vapor temperature and pressure, which forces the boiling to continue (and thus some nucleation sites to remain active) as long as possible. If the heat input resumes before the last large nucleation site quenches, a well-behaved restart will occur. The drawback of this approach is that it is an active method, requiring additional controls logic. It also subjects the receiver to wider temperature variations during cloud transients than the passive method.

As in the discussion of designing for stability, the point here is that there are no reliable tools for the design of an alkali-metal boiler that will have good hot restart behavior. Some questions that can be posed are:

1. Is there an optimum gas or gas mixture to control hot restarts?
2. Is there an optimum gas pressure?
3. What is the effect of orientation?
4. What is the effect of configuration?
5. In the added-gas method, what mechanism controls hot restart behavior?

2.3.3 Heat Transfer Crises

In addition to boiling instability and the hot-restart problem, there are two crises in heat transfer that can affect the liquid-metal reflux receiver. They are transition to film boiling, and flooding. These two phenomena are local and global aspects of the same problem: failure of liquid to return to the absorber because of the departing vapor flowrate.

Transition to film boiling occurs when the heat flux to the absorber exceeds a critical value (CHF). The transition may occur from either nucleate boiling or from liquid-phase natural convection [24]. Unfortunately, there have been very few measurements of the CHF for sodium, and only one for

NaK-78 [25]. These CHF's (as a function of operating temperature) are the only tools available for designing to avoid film boiling. Among the unsettled questions are the effect on CHF of: (a) heated-surface orientation, (b) added gas, and (c) subcooling [26].

Flooding occurs when at a given temperature the vapor transport of heat in the passage between the heated surface and the condenser exceeds a critical flux. Current design practice is to size the vapor-flow passage according to Kutateladze's correlation of flooding conditions, which is based on results from ordinary liquids in vertical cylinders [27,28]. Recently, this correlation was partially validated for NaK in a cylindrically-symmetric bench-scale test [14].

From this outline, it is clear that design tools for the avoidance of heat transfer crises in boiling liquid metals are less than adequate. This is particularly so for the reflux receiver, with its complex geometry, varied orientations, and transient operating conditions. The burnout experienced with the first pool-boiler receiver did in fact occur during a transient. The design tools suggest that either transition to film boiling or flooding may have occurred. The design of the 2nd-generation pool-boiler receiver provides for lower fluxes and larger vapor-flow passage dimensions. Because shape and orientation are likely to be important, and scaling laws are unproved, tests to establish heat flux limits are best done on the full scale device. In contrast to the quartz-lamp-heated bench-scale boilers, the entire absorber surface can easily be monitored for localized overtemperature, using a scanning infra-red camera.

3 Test Objectives

The overall test objective was to bench-test qualify heated-surface modifications and/or noncondensible-gas additions for use with NaK-78 in a Haynes Alloy 230 pool-boiler solar receiver. Qualification was based on boiling stability and hot-restart behavior at temperatures up to 750^{o}C. A secondary objective was to improve the pool-boiler design tools by modifying tests and adding tests as appropriate to further develop our understanding of boiling liquid-metals behavior.

4 Test Design

4.1 Bench-Scale Boilers

The bench-scale boilers were all of the same basic design shown in Figure 8. The design evolved out of our earlier sodium bench-scale tests [10]. The present boilers were fabricated from Haynes Alloy 230. The welded-seam tubing had an outside diameter of 1.75 inches and a wall thickness of

0.049 inches. It was custom made for us by Valley Metals of El Cajon, CA. The end caps were made from 1/8-inch sheet. Thermowells in the end caps were made from 1/8-inch x 0.028-inch-wall Inconel-600 (IN600) tubing, to accommodate 1/16-inch sheathed thermocouples. Tubes with valves were connected to the boiler bottom cap for vacuum pumping and liquid-metal filling. The outside diameters of the tubes were 1/2 inch and 1/4 inch respectively.

All of the parts were joined using autogenous welds back-purged with argon. Modifications to the wetted side of the heated surface for boiling stabilization were made before the bottom cap was welded to the boiler. Also at that time, flattened Type-K IN600-sheathed thermocouples were furnace-brazed to the air side of the heated surface. The heated surface was situated as far away as possible from the weld seam in the 1.75-inch tube. This was done to avoid non-reproducible nucleation sites that might reside in the weld. A strip of 0.004-inch thick zirconium foil was used in the boiler as an oxygen getter. The strip, 1 x 12 inches, was corrugated and then rolled into a 1-inch high cylinder. The cylinder was inserted into the lower end of the boiler before the bottom cap was welded on.

The boilers were leak checked using a helium mass spectrometer. They were vacuum baked at 600°C for 24 hours and then leak checked again using the vacuum system residual gas analyzer. With a helium-leak sensitivity of at least 0.5×10^{-8} cc/sec, no leaks were detected.

The liquid metals (NaK-78 and in one case sodium) were high-purity grades obtained from Callery Chemical Company of Callery, PA. They were purchased in 25-pound lots shipped in stainless-steel containers with an argon cover gas. The sodium was melted and heat soaked as described in a previous report [10]. Both the sodium and the NaK-78 were pushed by the cover gas from the shipping container into the benchscale boiler through an all-metal manifold. The cover gas pressure was maintained by adding high-purity argon to the shipping container as required. To determine when the desired liquid-metal transfer was complete, the pool level was detected by 4-wire resistance measurements across the boiler diameter.

Gas was added or removed from the boilers using the following method: first, the boiler was inverted. Then the 1/2-inch valve was connected to an all-metal gas-transfer manifold, which in turn was connected to a turbomolecular vacuum-pump station. With the valve closed, a high vacuum was established from the pump station to the valve by vacuum baking. Then the closed valve and the tube connecting it to the boiler end cap were evaporatively cleared of liquid metal by heating to between 400 and 450°C for 24 hours. The valve was then opened and the gas in the boiler sampled by a residual gas analyzer at the pump station. The boiler could be re-evacuated and/or gas could be metered in through the gas-transfer manifold. The fill gas pressure was measured using a capacitance-type gauge.

Liquid metal was removed from the boilers on several occasions: twice for boiler modifications, and once, to replace NaK-78 with sodium. To remove the metal the boiler was again inverted. Then, the 1/4-inch valve was connected to a tee. The side leg of the tee was connected to a 1/4-inch valve leading to a vacuum-pump station. The bottom leg was connected to a 1/4-inch valve leading to an empty liquid-metal waste can. Vacuum was established from the pump station up to the closed valve on the boiler. Then the valve on the side leg of the tee was closed and the valve on the bottom leg of the tee was opened to drain the boiler into the waste can. The boiler was heated to between 450 and 575°C and connections to the waste can were heated to between 225 and 300°C for 52 hours to evaporate the remaining residue out. The end cap and valves were then cut off. The boiler was cleaned with water. After the modifications were made, a new getter was inserted and a new end cap and valve assembly was welded on.

4.1.1 Initial Set of Four Boilers

The surface-modification details of the initial set of four bench-scale boilers were as follows:

1. Unmodified (baseline boiler).
2. A laser-drilled cavity approximately 0.008" diameter at the mouth and 0.018" deep (typical cross-section shown in Figure 6).
3. One 1/4-inch patch of hot-press-sintered IN600 -100/+140 powder (typical cross-section shown in Figure 7).
4. One 1/4-inch patch of hot-press-sintered 304L stainless-steel -100/+140 powder.

The development details of these modifications have been presented in a previous report [29]. Schematics of their placement are shown in Figure 9.

4.1.2 Second Set of Four Boilers

After a disappointing outcome from the first four surfaces, a second set of bench-scale boilers was prepared for the same test objectives. These boilers had the following heated-surface modifications:

5. Heat input and surrounding area covered by hot-press-sintered 304L stainless-steel -100/+140 powder. This coating was applied by Thermacore, Inc. of Lancaster, Pennsylvania using a proprietary process.

6. Heat-input area covered by type-304 stainless-steel powder coating. A typical cross section is shown in Figure 10. A single boiler had three different coated areas at 120° azimuthal intervals (powder mesh sizes of -60/+80, -80/+100, and -100/+150 respectively). During testing, each area in turn was centered in front of the lamp assembly. The coatings were applied by Friction Coating, Inc. of Sterling Heights, Michigan, using a proprietary process that does not require applied pressure. The coatings were tested at Sandia for interfacial strength using the same methods and criteria that were applied to items 3 and 4 above.

7. Heated surface with EDM cavities. Two cavities were spaced such that one or the other or both could be within the heated area. We built this boiler to test with NaK, which we had not previously done, as well as to test with sodium to make replicate our earlier successful on-sun work. A typical cavity is shown in Figure 11.

8. IN600 patch from item 3 above, with an overlay of 56-mesh stainless-steel screen spot-welded in place. This modification was based on the idea that some damping of liquid motion next to the heated surface might inhibit nucleation-site quenching.

Schematics of the placement of these modifications are shown in Figure 12.

4.2 Test Apparatus

The bench-scale tests were carried out in the Engine Test Facility of Sandia National Laboratories' National Solar Thermal Test Facility (NSTTF). The test apparatus included:

1. A 6000-Watt quartz-lamp assembly (Figure 13) made by Research, Inc. of Minneapolis, MN. The lamp assembly is used to heat the liquid metal pool in the boiler.

2. A water-cooled gas-gap calorimeter to cool the condenser end of the boiler (the gas gap contains a helium/argon mixture that serves as a variable thermal resistance to control the boiler temperature).

3. A test stand (Figure 14) to hold the boiler, lamp assembly and calorimeter at various angles relative to vertical.

4. Control systems for lamp power and for the calorimeter gas mixture. The lamp-power control determines the input power to the boiler. The calorimeter gas-control system determines the boiler temperature required to transfer this power to the calorimeter.

5. A data-acquisition system.

The calorimeter, control system, and data-acquisition system have been described in detail previously [30]. An overall schematic of the test is shown in Figure 15. Not shown are the multiple layers of refractory ceramic fiber blanket used to insulate the entire test vessel against thermal losses to the surroundings.

4.3 Test Procedure

Our test procedure was tailored to the objectives outlined in Section 3. The following test hierarchy was adopted : (1st) boiling-stability tests without added gas, (2nd) hot restart tests without added gas, (3rd) stability tests with added gas, and (4th) hot-restart tests with added gas. Deviations occurred for a variety of reasons. The main reason was that in some cases stable boiling was not obtained. In such cases hot-restart testing was not pursued, because without stability, hot restart tests could not be staged in a repeatable fashion. Other less-common reasons for deviations will be identified as they arise in the remainder of this report.

The boiling-stability test sequence that we used is shown in Figure 16. Consistency over the full range of test conditions and test specimens was not possible. Some surface modifications were not fully characterized because they were only included to make contact with previous work. Deviations from the test sequence occurred as a result of unstable boiling, equipment problems, and resource limits. The sequence also evolved somewhat as the tests proceeded -- for example, to define the limits of stability when boiling behavior was very good, the sequence had to be extended to less stable conditions (lower power and temperature as predicted by Shai and Rohsenow's stability theory). Another change affected tests with heated-surface tilt out of the vertical -- these were routinely conducted in the beginning, but much less often once the effect of tilt was established. To keep the size of the test matrix manageable, the amount of gas that was added to the boilers was usually fixed at a single pressure (0.37 torr). Higher pressures were shown to interfere with condensation heat transfer.

The test sequence for hot-restarts is shown in Figure 17. Not shown is the provision to repeat any well-behaved hot restart a minimum of three times. This sequence is patterned after the hot-restart tests conducted on the first on-sun pool-boiler receiver. All of the discussion with regard to consistency in the preceding paragraph applies as well to the hot restart tests.

5 Results and Discussion

An overview of the complete set of data that is recorded during each test is presented for one particular stable boiling run as follows:

1. Boiler indicated temperatures -- surface, liquid and vapor -- (Figures 18-21)
2. Calorimeter and lamp-housing cooling-water flow rates (Figure 22)
3. Calorimeter cooling-water inlet and rise in temperature (Figure 23)

4. Calorimeter cooling-water temperature change as measured by a thermopile (Figure 23)
5. Lamp-housing cooling-water and lamp cooling-air outlet temperatures (Figure 24)
6. Calorimeter argon and helium flow rates (Figure 25)
7. Lamp-array power supply control voltage and three-phase currents -- one phase per lamp pair -- (Figure 26). The currents are approximately proportional to the control voltage -- power was customarily set as "percent of full power" by setting the voltage at the same percent of 5 volts.

The data rate is varied during the test as required by the test engineer. The rate is typically once every 5 seconds at startup and during steady operation and once every 30 seconds during cool down. Figure 27 shows the boiler throughput power computed from the calorimeter data. This result is computed in real time and recorded along with the data. Most of the data are used by the control system to determine if the system is operating safely or if a safety-required automatic shutdown should be executed. Data are recorded to help: (a) characterize boiling behavior, (b) diagnose the cause of shutdowns, and (c) explain unexpected behavior.

The test results of most interest in the present case are heated-surface and condenser temperatures shown as a function of time. These adequately characterize both boiling stability and hot restarts. In the following subsections at least one such set of temperature-time histories is presented for each test.

5.1 Initial Four Boilers

Test results from the first four boilers are presented in Figures 28-41. Results from the boiler with the laser-drilled hole are presented in Figures 28-31. In Figure 28, the boiler was run in the vertical position (0^{o}), then tilted $+30^{o}$ and $+60^{o}$ out of the vertical, and then returned to 0^{o}. Positive tilt (e.g. $+30^{o}$) denotes heating from below. A number of boiling-cessation events are evident, with heated-surface temperatures rising over $100^{o}C$ and automatic safety shutdowns occurring. With the boiler tilted, the stability is better but still not acceptable. Figure 29 shows the dramatic improvement with 1.5-torr of added xenon. Figure 30 shows equivalent results with the xenon pressure reduced by a factor of four. In each case there still were cessation-of-boiling events. Figure 31 shows the effect of xenon on the temperature drop from the pool to the condenser. This temperature drop increases as the xenon pressure increases. In a dish/Stirling system this loss of available temperature would cause the engine to operate less efficiently. Figures 29-31 are the basis for using the lower xenon pressure in most of the other boiler tests.

Results from the boiler with the IN600-powder-coating patch are presented in Figures 32-34. Again, boiling was unstable in the vertical position, and improved but not acceptable at +30, +60^{o} or with added xenon . Figure 34 shows the less-stable behavior observed when the xenon was removed and replaced by helium.

Results from the boiler with the Type-304L stainless-steel powder-coating patch are presented in Figures 35-38. Once more, boiling was unstable in the vertical position and improved but still unstable with positive tilt or added xenon. Figure 37 shows substantially the same result with negative tilt (heating from above). Figure 38 suggests that stability is better with *sideways* tilt, but we cannot say that cessation of boiling would not have occurred in a longer test.

Figures 39-41 show the results for the baseline boiler (unmodified heated surface). The trends in Figures 39-40 are similar to those seen with the surface modifications, and suggest that none of the modifications affected a significant improvement. The test shown in Figure 41 was motivated by questions raised in earlier work regarding the effect of oxygen contamination [31]. In that work, we speculated that oxygen contamination might have occurred and might account for an unexplained improvement in boiling stability. The xenon was pumped out of the baseline boiler and 50 ppm of oxygen was added. We recognize that the oxygen concentration probably decreased during the test -- based on published rates [32], we estimate that the zirconium getter reduced the oxygen concentration to about 25 ppm in the first 7 minutes at 650^{o}C, and to 10 ppm after 30 minutes. However, the boiling stability shown in Figure 41 is poor throughout the test. A Comparison of Figures 39 and 41 suggests that 50 ppm of oxygen does not improve boiling stability.

Hot-restart tests were not attempted with any of the first four boilers because boiling stability was not acceptable.

5.2 Second Four Boilers

Test results from the second four bench-scale boilers are presented in Figures 42-51. The boiler coated by Thermacore, Inc. was tested first. In contrast to the disappointing results from our first four boilers, Thermacore had demonstrated stable boiling in a bench-scale boiler using their coating [14]. They used induction heating over a larger area that spanned the full circumference of the boiler tube. After the disappointing results from our first four boilers, making contact with the Thermacore work was a high priority. We were particularly interested in the possibility of hidden variables that might lead to different test results at the two laboratories. Figure 42 shows the results from the Thermacore-coated boiler. The stability is very much better than we observed with our first four boilers at the same conditions. Several cessation-of-boiling events are apparent (rapid excursions of over 100^{o}C at the start and finish of each run). This is contrary to Thermacore's experience. The explanation for these differences was explored in follow-up tests described in Section 5.3.

Figure 43 shows results with the -80/+100 powder applied by Friction Coatings, Inc.. They appear to be equivalent to what we saw with the Thermacore coating. Figures 44 and 45 show additional tests with the -80/+100 coating, including both boiling runs and hot restarts in the vertical position and with +30^{o} tilt. Cessation-of-boiling events can be seen during boiling at the lower temperatures. All of the hot restarts required large wall superheats to initiate boiling. Boiling stability was slightly better with the -60/+80 coating and slightly worse with the -100/+150 coating (not shown). We cannot say that these differences are inherent in the coatings -- they may depend on the order in which the coatings were tested, since the coatings are all in a common pool of liquid metal and surface chemical changes that may affect the results continue through each test. The results may also be misleading because of the random nature of the events and the limited test time. This point is illustrated in Figure 46, which corresponds to a repeat of the test shown in Figure 43: a solitary boiling-cessation event is seen in Figure 43, illustrating the random nature of the results; an increased number of events is seen in Figure 46, which could be a result of cumulative test time. The improvement with 0.37 torr of xenon is presented in Figure 47. There is still some cessation of boiling during the starting transient, but in contrast to all of the previous tests, the rest of the run was flawless. Figure 48 shows hot restarts performed with this system, followed by a stable boiling run extended to even lower temperatures. The addition of xenon improved hot-restart behavior -- some though not all of the restarts in Figure 48 were accomplished without significant wall superheat. Boiling stability and hot-restart behavior were not quite as good at +30^{o} and -30^{o} tilt (not shown).

Additional hot restart tests (not shown) were performed using the -60/+80 and -100/+150 coatings with 0.37 torr of added xenon, and using the -80/+100 coating with (a) 0.37 torr of xenon mixed with 0.37 torr of helium, (b) 10 torr of xenon, and (c) 10 torr of helium. No significant differences in hot-restart behavior were seen between these various tests, or between these tests and the previous ones.

The failure to achieve good hot-restart behavior after the addition of noncondensible gas is at odds with Thermacore's bench-scale tests using NaK-78 and our on-sun tests using sodium. To explore this puzzle we next shortened the Friction Coatings boiler from 36 inches to 24 inches (the pool depth was unaffected). The rationale was as follows. The on-sun tests led us to suspect that good hot-restart behavior was obtained by gas entrained in the liquid metal [7]. Entrainment occurs when liquid from the pool is thrown into the gas that has been swept to the rear of the condenser. In our bench-scale boilers, we hypothesized that the aspect ratio might inhibit this action (in a long thin tube, only droplets ejected from the pool within a small solid angle will reach the opposite end). The results with the shortened tube are shown in Figure 49: most of the restarts are well behaved, in support of our hypothesis.

The third bench-scale boiler to be tested was the one with two electric-discharge-machined (EDM) cavities. In its first test, the boiler was positioned so that only the lower cavity was in front of the lamps. Boiling was very unstable. Analysis of the heated-surface temperatures determined that the boiler was mechanically ratcheted upward by the accompanying mechanical shocks combined with frictional constraints. After the boiler was secured to prevent further ratchetting, it was tested with both cavities in the heat-input zone. Boiling was still very unstable, and mechanical shocks to the upper end cap eventually caused a leak. The test results, shown in Figure 50, are surprising since the cavity depth was believed to be deep enough to ensure stability. The bench-scale boiler was drained, cleaned, repaired, and filled with sodium to make contact with our on-sun tests -- in which a boiler with EDM cavities and filled with sodium demonstrated very stable boiling. No improvement in stability was obtained.

The last boiler tested was the one in which a screen mesh had been spot welded over the existing small IN600 powder-metal patch. The stabilizing effect of the screen, while not complete, is evident in a comparison of results before and after its addition to the boiler (Figures 32 and 51).

5.3 Follow-up Tests

Several follow-up tests were run using the Thermacore-coated tube. There were two objectives:

1. Assess the effect of heat-input surface area on boiling stability.
2. Measure the pressure in the boiler during NaK-78 boiling.

5.3.1 Effect of Area on Boiling Stability

The investigation of the effect of heated-surface area on boiling stability was motivated by the following observations:

1. Boiling stability seemed to improve with increasing powder-metal-coating area -- progressing from our 1/4" patch to our fully-covered 1" x 4" heated area to Thermacore's fully-covered 2" x 9.4" heated area.
2. Boiling in the baseline boiler (no surface modification) improved dramatically with tilt.
3. Boiling in the bench-scale boiler with EDM cavities was not stable, whereas in the previous on-sun full-scale test with EDM cavities, boiling was stable.

The improvement in stability with increasing area might be explained by intrinsic differences in the coatings. On the other hand, it could be a consequence of size alone. This could be explained as follows: suppose a small heated patch is marginally unstable because it has only one nucleation site, which on average inflates N bubbles before it is deactivated. Now suppose the patch is enlarged to include two such nucleation sites. When one site deactivates, boiling action from the other may reactivate it [33]. The sites will *simultaneously* deactivate on average only once every N^2 bubbles -- total cessation of boiling thus occurs much less often, which is to say that stability is greatly improved.

Taken together, the observations listed above suggest that boiling stability in the full-scale boiler may have occurred not because of the EDM cavities but rather as a result of factors such as area and orientation. This would have immediate practical application. It would also imply new mechanisms for inclusion in any model of boiling stability. The Thermacore-coated tube was selected for this follow-up test because of its large coated area. We used a second lamp assembly to double the heated area. In the first test the lamps were vertically stacked as illustrated in Figure 52 (the light shield shown in the illustration was used in a subsequent test). The quartz windows on the front of the lamp assemblies were located 2 inches from the boiler so that the heated areas overlapped. In all of the previous tests, the window was 1/4 inch from the boiler. We estimate that the change in position lowered the peak flux on the boiler from 92 W/cm^2 to about 30 W/cm^2. Three boiling runs were conducted sequentially: first with the upper lamp assembly alone, second with both assemblies, and finally with just the lower assembly. The test results are shown in Figure 53. The three runs should be compared mindful of differences in temperature and heat flux, since the stability criteria of Shai and Rohsenow depends on both [8]. For example, compare the 12 minutes with only the upper lamp array on, at full power, beginning at 8:50 (unstable), and the 12 minutes with both lamp arrays on at 3/4 power, beginning at 9:30 (stable). This comparison is appropriate because (a) the operating temperatures are the same and (b) according to the Shai and Rohsenow stability theory, the relative stabilities should not have changed even if the power was increased in the second run. Following this reasoning, the results shown in Figure 53 confirm that boiling stability improves with heated-surface area.

Will increasing the heated area improve stability if the new and old areas are not contiguous? To answer this, we divided the overlapping heated areas with a 1/2-inch-wide water-cooled shield as illustrated in Figure 52. For this test the lamp controls were modified so that we could control the two lamp assemblies independently during a boiling run. We were then able to switch from one to two lamp assemblies and back, in one continuous run. The results are shown in Figure 54. They show stable boiling whenever both lamp assemblies were on, regardless of which was turned on first.

The tests with the vertically-stacked lamp assemblies indicate that boiling stability improves with increasing heated-surface area. Apparently the new area does not have to be contiguous to the old one. Left unanswered is how far apart the areas may be and whether or not they must be situated one above the other to be effective. To address these questions, a test was run with the lamp assemblies placed on opposite sides of the boiler and the windows 1/4" from the heated surfaces, as shown in Figure 55. To make the input heat flux about the same with the closer lamp spacing, the percentage of full power is lower than with the stacked lamps. The additional heated surface was instrumented with intrinsic Type K thermocouples for this test. The results are shown in Figure 56. They indicate that mutual enhancement of boiling stability did not occur with the lamps on opposite sides. In Figure 56, cessation of boiling *appears* to occur on both heated surfaces simultaneously in every instance. However, it is likely that boiling initiated on one surface, and the resulting turbulent cooling prevented boiling initiation on the opposite side. Thus what is seen is probably the stability characteristic of a single surface. In a hybrid receiver where one surface is solar heated and a second is gas fired, this kind of behavior could lead to problems akin to a hot restart as the heat input is shifted from one surface to the other. With the vertically-stacked lamps it appears that the behavior was dominated by nucleation sites on one surface being activated by boiling action on the other surface.

5.3.2 Boiler Pressure Measurement

The measurement of boiler pressure during NaK-78 boiling was motivated by concerns raised when our long-term (10,000 hour) bench-scale test was started. The long-term bench-scale boiler is nearly identical to the shortened Friction-Coatings-modified boiler described in Section 4.1.2.

One difference is a strain-gauge pressure transducer connected to a tee in the 1/4" fill tube. It was added to detect leaks that might occur during long-term unattended operation. The vapor pressure of NaK-78 at operating temperature is subatmospheric: 10.3 psi at 750°C versus 12.12 local atmospheric pressure [34]. Thus, a leak is indicated if the measured pressure -- corrected for the pool hydrostatic head -- exceeds 10.3 psi.

During trial runs of the long-term test, the indicated vapor pressure was much higher than expected. In fact, it was close to the vapor pressure of potassium over a wide temperature range. The pressure transducer was not suspected because its calibration had been checked before the test began. Rechecking the calibration was not attempted -- it would have required removing the transducer from the sealed liquid-metal system, a very difficult exercise. Because the vapor pressure was close to that of potassium, we looked for a phenomenological explanation.

Others have measured the vapor pressure of NaK over a range of temperatures and confirmed that it follows Raoult's law [34]. That is, they have confirmed that the partial pressures in the vapor mixture are the pure-substance vapor pressures times their respective liquid mole fractions ($P_{NaK} = \chi^l_{Na} P_{Na} + \chi^l_K P_K$). Applying the ideal-gas law shows that the vapor is potassium enriched ($\chi^v_{Na} = \chi^l_{Na} P_{Na} / P_{NaK}$, $\chi^v_K = \chi^l_K P_K / P_{NaK}$) [35]. It follows that the liquid left behind when a bubble is inflated will be sodium enriched. Because sodium is denser than NaK-78, it will tend to settle to the bottom of the boiler. Turbulent mixing and mass diffusion oppose this tendency. In our particular boiler, we could not dismiss the possibility that the large heat throughput would quickly result in segregation of the sodium from the refluxing cycle to the dead volume below the heat-input region.

To test for this possibility, we modified the Thermacore-coated boiler. Four-wire resistance probes were spot-welded to the boiler to detect sodium enrichment in the dead space and potassium enrichment in the heated zone. Each four-wire set consisted of a pair of wires used to pass a 5-amp dc current across the boiler diameter, and an adjacent pair to monitor the resulting voltage. A calibrated strain-gauge pressure transducer was mated to the boiler fill valve. The space between the valve and the transducer was evacuated and the valve was opened to allow the transducer to sense boiler pressure. A simple boiling run at full power up to 750°C was executed. The resistance-probe voltages, smoothed for clarity of presentation, are shown in Figure 57. Also shown are calculated voltages for NaK-78, sodium and potassium. The time-variation of the calculated voltages is a consequence of the temperature dependence of the liquid-metal electrical resistivities. The measured voltages are in best agreement with the voltage variation calculated for NaK-78, suggesting that separation did not occur. More significantly, the indicated pressures are in agreement with the values expected for NaK-78, as shown in Figure 58. This result led to the discovery that the transducer in the 10,000-hour test had been incorrectly wired after the calibration check when temporary cables were replaced by permanent ones.

These measurements laid to rest concern that the published values of NaK vapor pressure are inapplicable in our boiler. Boiler pressure in the 10,000 hour test will be subatmospheric at 750°C and the pressure transducer can be used to detect a breach as planned.

5.4 Flash Radiography

A secondary objective of the bench-scale screening tests was to improve the pool-boiler design tools by modifying tests and adding tests as appropriate to further develop our understanding of boiling liquid-metals behavior. Some activities of this sort were described in Sections 5.3.1 and 5.3.2. In addition, towards the end of our test series we had the opportunity to use flash radiography for imaging bubbles in a bench-test pool boiler. To our knowledge, such measurements in alkali metals have been conducted only once before, by Bobrovich et al with potassium [36].

The information that can be derived from flash-radiography imaging includes bubble size, bubble spacing, and nucleation-site locations. Combining the bubble spacing with bubble-rise velocity (which may be available from correlations) gives the bubble frequency. Elements of boiling theory that predict bubble size and frequency can be checked against the measured values. Also, the heat transfer carried by convection can be estimated from bubble size and frequency -- this is a quantity used by Shai and Rohsenow in their stability model [8]. Finally, the determination of nucleation-site locations can be useful in developing better stability theories. It can also settle the question of whether boiling on one heated surface suppresses boiling on a second, a question raised in Section 5.3.1.

We used the Thermacore-coated tube because it was already mounted in the test stand and could produce stable boiling. The flash X-ray system was a Hewlett Packard Model 43734A. This system provides a nominal 25-nanosecond pulse of 450-kV X-rays, resulting in a 20-mR dose per pulse at 1 meter. The film was Dupont NDT 57 industrial radiographic film with Dupont NDT Hi-Plus intensifying screens front and rear, in 14" x 17" medical cassettes. The physical arrangement and dimensions are shown in Figure 59. A remote-control cassette changer was used to make four exposures before the test. The cassettes were replaced and four exposures were made during boiling: two at 650°C and two at 700°C.

The exposures made during boiling were enhanced by digital image manipulation. Both the pretest and test images were digitized using a 76-μm square spot size. The images were manipulated using the Macintosh application "IPLab Spectrum", by Signal Analytics of Vienna, Virginia. The pretest image was dimensionally scaled and rotated to match the test image. The images were then subtracted and contrast-enhanced to yield the results shown in Figures 60-63. As a result of slight positional mismatches, the subtraction technique did not eliminate fine features such as the wires holding the insulation blankets in place, or the sheathed thermocouples. It did eliminate larger features that might be interpreted as bubbles -- for example, voids in the insulation. The images shown in Figures 60-63 are considerably less clear than they were on the video display. Their interpretation is admittedly subjective. Our identification of bubbles, shown as white tracings in the figures, yield bubble diameters on the order of 1.5 cm at both 650°C and 700°C. The vapor pressures corresponding to these temperatures are 3.6 and 6.2 psia (186 and 320 torr). Figure 64 compares our bubble-diameter estimates with the results of Bobrovich et al and with the correlation of Cole and Rohsenow as presented in Dwyer's book [37]. Our estimates are smaller than Bobrovich's results and equal or larger than the correlation. Consistent with Bobrovich's results, they do not have the correlation's dependence on pressure. Bobrovich boiled potassium on smooth-surfaced horizontal rod heaters, while we boiled NaK-78 on the powder-metal-coated internal surface of a vertical cylinder. Our minimum boiler dimension was about 2/3rds Bobrovich's. It is not known if these differences can account for the difference in bubble diameters. Figure 60 is especially interesting, because it seems to show a lens or mushroom-shaped bubble in the process of inflating at the lower end of the heated surface, thus locating an active nucleation site.

The x-ray images suggest that heat transfer through the pool may be dominated by sensible-heat convection, as follows. The total amount of latent heat in the vapor volume of these images is rather small: it can be calculated from the latent heat times the estimated total vapor volume divided by the specific volume of the vapor. The latent heat is roughly 2440 J/gm between 650 and 700°C. Our estimate is that the total vapor volumes are all on the order of 45 cm^3. The specific volume is about 15200 cm^3/gm at 650°C and 8300 cm^3/gm at 700°C. Thus the total latent heat in the vapor volumes is about 7.2 J at 650°C and13.2 J at 700°C. The height of the images is 0.73 ft and the throughput power at both temperatures was about 1250 W_t, so that for all of the power to be transported as latent heat, the bubble rise velocity would have to be (1250/7.2)x0.73 = 127 ft/s and (1250/13.2)x0.73 = 69 ft/s respectively. Values very much larger than 1 ft/s are unlikely [38], indicating that sensible-heat convection may be dominant in the pool (we estimate that this only requires a liquid-velocity superheat product of 10 ft-°C/s). Because of the importance of this possibility both for boiling-stability criteria and for internal dynamics such as flooding, further study is warranted before a definite conclusion is drawn. In particular, direct confirmation of bubble velocities by x-ray cinematography is recommended.

6 Summary and Conclusions

Bench-scale screening tests were conducted in support of the design of a 75-kW_t solar pool-boiler receiver made from Haynes Alloy 230 and containing the sodium-potassium alloy NaK-78. Quartz-lamp-heated boilers were used to screen candidate boiling-stabilization materials and methods at temperatures up to 750°C. Candidates that provided stable boiling were tested for hot-restart behavior. A secondary objective was to improve the pool-boiler design tools by modifying tests and adding tests as appropriate to further develop our understanding of boiling liquid-metals behavior. Towards this end, the effect of heated-surface area was studied using two lamp assemblies run separately and together. Also, flash radiography was used to estimate the size of bubbles formed during boiling.

The following conclusions are drawn:

1. Unstable boiling occurred with the small surface modifications (1/4" sintered patches, laser-drilled holes, electric-discharge-machined holes).

2. Unstable boiling continued to occur with the electric-discharge-machined holes when sodium was substituted for NaK. This indicates that stable boiling in the first full-scale receiver was a consequence of other factors than (or in addition to) the EDM holes.

3. The most stable boiling occurred with the larger surface modifications (1" x 4" Friction Coatings, Inc. patches and Thermacore coating).

4. The addition of 1.5 torr of xenon improved stability but interfered with heat transfer at the condenser. The addition of 0.37 torr of xenon stabilized boiling as well without affecting heat transfer. The effect of added gas was most pronounced on the least-stable systems.

5. Neither the addition of 0.37 torr or 10 torr of helium improved stability.

6. Tilt of the heated surface out of the vertical improved poor stability.

7. Hot-restart behavior was poor in all cases. It was improved but still unacceptable with the addition of 0.37 torr of xenon. Higher pressures of xenon and additions of helium up to 10 torr did not lead to further improvement. The fact that the results were better with xenon than with helium are evidence that hot-restart improvement is dominated by entrainment rather than precipitation of dissolved gas.

8. When the boiler was shortened from 36" to 24" the hot-restart behavior with added gas improved but was still unacceptable . This result is consistent with the earlier on-sun experience, and is further evidence that entrainment is the dominant mechanism in hot-restart improvement.

9. Boiling stability was improved when the heated-surface area was increased by adding a second lamp assembly in a vertically-stacked configuration. This was the case even when the heated-surface area was divided into two adjacent but non-contiguous parts by a water-cooled light shield.

10. Boiling stability was not improved when the heated-surface area was increased by adding a second lamp assembly opposite the first.

11. With two lamp assemblies on opposite sides of the boiler, it appears that boiling on one heated surface suppresses boiling on the other. This does not appear to be the case when the lamps are stacked vertically. This may be important in the design of hybrid receivers.

12. Items 2-4, 6 and 9 strongly suggest that stable boiling of alkali metals may be achievable in a full-scale receiver without any heated-surface modifications.

13. Flash radiography with digital image subtraction and contrast enhancement was used to estimate bubble size and shape in bench-scale NaK boilers. The estimated bubble sizes are equal or larger than theory predicts and independent of pressure, consistent with the only other measured values.

14. The x-ray images suggest that convective transport of sensible heat may be the dominant heat-transfer mode in the liquid-metal pool. This warrants further study, perhaps using x-ray cinematography.

15. Flash radiography may be useful in determining the location of active nucleation sites and in answering questions such as whether or not boiling on one surface is suppressing boiling on a second area.

References

[1] Bean, J.R., and Kubo, I., "Development of the CPG 5 kW Dish/Stirling System," Paper No. 906298, Proceedings of the 25th IECEC, Reno, NV, 1990.

[2] Diver, R.B., Andraka, C.E., Moreno, J.B., Adkins, D.R., and Moss, T.A., "Trends in Dish Stirling Solar Receiver Design," Paper No. 905303, *Proc. of the 25th IECEC*, Reno, NV, 1990.

[3] Laing, D., and Goebel, O., "Sodium Heat Pipe Solar Receiver for a SPS V-160 Stirling Engine: Development, Laboratory and On-Sun Test Results," Paper No. 915363, *Proceedings of the 26th IECEC*, Boston, MA, 1991.

[4] Andraka, C.E., Diver, R.B., Adkins, D.R., Rawlinson, K.S., Cordeiro, P.G., Dudley, V.E., and Moss, T.A., "Testing of Stirling Engine Solar Reflux Heat-Pipe Receivers," Paper No. 93IEC-295, *Proceedings of the 28h IECEC*, Atlanta, GA, 1993.

[5] Moreno, J.B., Andraka, C.E., Diver, R.B., Ginn, W.C., Dudley, V., and Rawlinson, K.S., "Test Results from Full-Scale Sodium Reflux Pool-Boiler Solar Receiver," SAND89-2772C, Sandia National Laboratories, *Proceedings 12th ASME International Solar Energy Conference*, April, 1990, p. 95.

[6] Moreno, J.B., Andraka, C.E., Diver R.B., Moss, T.A., Hoffman, E.L., and Stone, C.M., "Reflux Pool-Boiler as a Heat-Transport Device for Stirling Engines: Postmortem Analysis and Next-Generation Design ," Paper No. 915355, *Proceedings 26th IECEC*, August 1991.

[7] Andraka, C.E., Moreno, J.B., Diver R.B., and Moss, T.A., *Sodium Reflux Pool-Boiler Receiver On-Sun Test Results*, SAND89-2773, Sandia National Laboratories, Albuquerque, 1992.

[8] Shai, I., and Rohsenow, W.M., "The Mechanism and Stability Criterion for Nucleate Boiling of Sodium," *Trans. ASME. Series C, J. Heat Transfer*, 91:315 (1969).

[9] Dwyer, O.E., *Boiling Liquid-Metal Heat Transfer*, American Nuclear Society, Hinsdale, Illinois, 1976, p. 207.

[10] Moreno, J.B. and Andraka, C.E., *Test Results from Bench-Scale Sodium-Pool-Boiler Solar Receiver*, SAND89-0899, Sandia National Laboratories, Albuquerque, June 1989.

[11] Saaski, E., Advanced Solar Conversion System (ASCS) Heat Transport System Working Group Meeting, Sandia National Laboratories, June 1989.

[12] Andraka, C.E., p. E-6.

[13] Andraka, C.E., p. D-29.

[14] Anderson, W.G., Rosenfeld, J.H., and Noble, J., "Alkali Metal Pool Boiler Life Tests for a 25 kWe Advanced Stirling Conversion System," Paper No. 915343, *Proceedings of the 26th IECEC*, Boston, MA, 1991.

[15] Andraka, C.E., p. E-7

[16] Romero, V. J., "CIRCE2/DEKGEN2: A Software Package for Facilitated Optical Analysis of 3-D Distributed Solar Energy Concentrators," *Proceedings ASME-JSES-KSES International Solar Energy Conference*, April, 1992, p. 961.

[17] Hogan, R. E. Jr., AEETES - Solar Reflux Receiver Thermal Performance Numerical Model," *Proceedings ASME-JSES-KSES International Solar Energy Conference*, April, 1992, p. 1015.

[18] Hoffman, E. L. and Stone, C. M., "Structural Analyses of a Dish Reflux Pool-Boiler Receiver," *Proc. ASME-JSES-KSES Int. Solar Energy Conference*, April, 1992, p. 1001.

[19] Dwyer, O.E., p. 4.

[20] Dwyer, O.E., p. 204.

[21] Dwyer, O.E., p. 210.

[22] Moreno, J.B., Andraka, C. E. and Moss, T.A., "Boiling Behavior of Sodium-Potassium Alloy in a Bench-Scale Solar Receiver ," Paper No. 929178, *Proc. 27th IECEC*, August 1992.

[23] Andraka, C.E., p. M-11.

[24] Dwyer, O.E., p. 404.

[25] Dwyer, O.E., p. 382.

[26] Dwyer, O.E., p. 411 and p. 401.

[27] Andraka, C.E., p. A-4.

[28] Rohsenow, W.M., Hartnett, J.P., and Ganic, E.N., eds., *Handbook of Heat Transfer Fundamentals*, McGraw-Hill Book Company, New York, N. Y., 1985, p. 13-24.

[29] Andraka, C.E., p. D-4.

[30] Moreno, J.B. and Andraka, C.E., pp. 15-24.

[31] Moreno, J.B. and Andraka, C.E., p. 49.

[32] Hinze, R.B., *Control of Oxygen Concentration in a Large Sodium System,* USAEC Report NAA-SR-3638, Atomics International, Dec. 1, 1959.

[33] Fauske, H.K., "Nucleation of Liquid Sodium in Fast Reactors," *Reactor Technology,* Vol. 16, No. 4, Winter 1972-1973, p. 294.

[34] Foust, O.J., Ed., *Sodium Nak Engineering Handbook*, Gordon and Breach, Science Publishers, Inc., 1979, Vol. 1, p. 59.

[35] Krell, E., and Lumb, E.C., "Handbook of Laboratory Distillation," Elsevier Publishing Co., Amsterdam, 1963, p. 66.

[36] Bobrovich, G.I., Avksentyuk, B.P., and Mamontova, N.N., "On the Mechanism of Boiling in Liquid Metals," *Proceedings Semi-Intern. Symp. Heat Transfer, Vol. 2*, Japan Society of Mechanical Engineers, Tokyo, September 4-8, 1967, p. 171.

[37] Dwyer, O.E., p. 184.

[38] Rohsenow, W.M., p. 13-18.

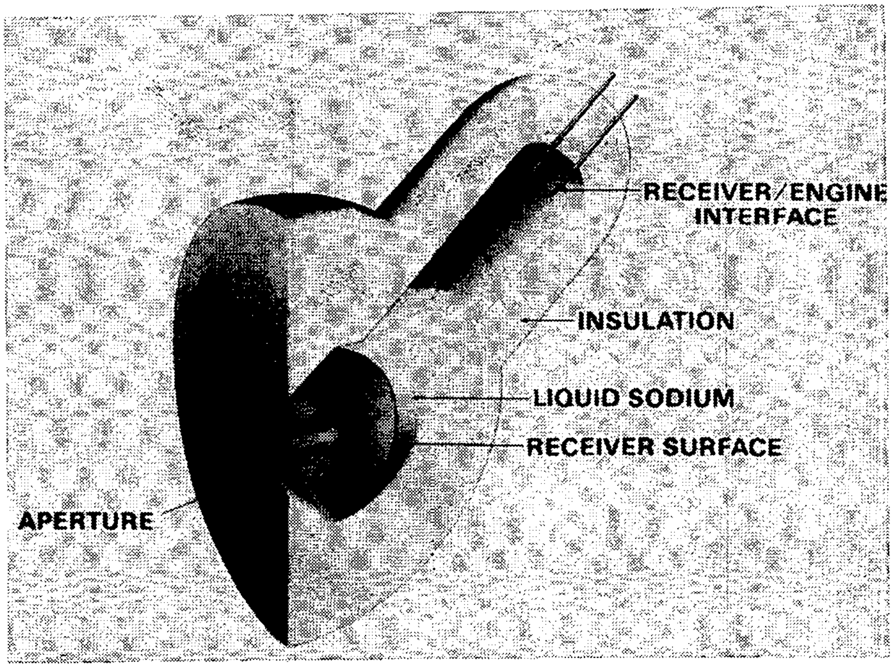

Figure 1. Schematic of first solar liquid-metal pool-boiler reflux receiver.

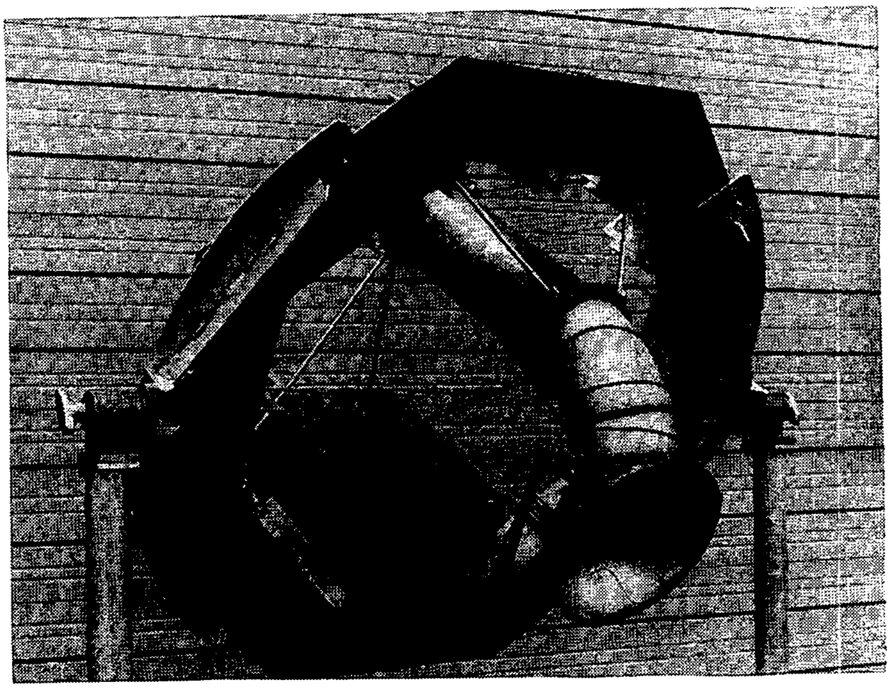

Figure 2. Photograph of first sodium pool-boiler receiver in its mounting ring.

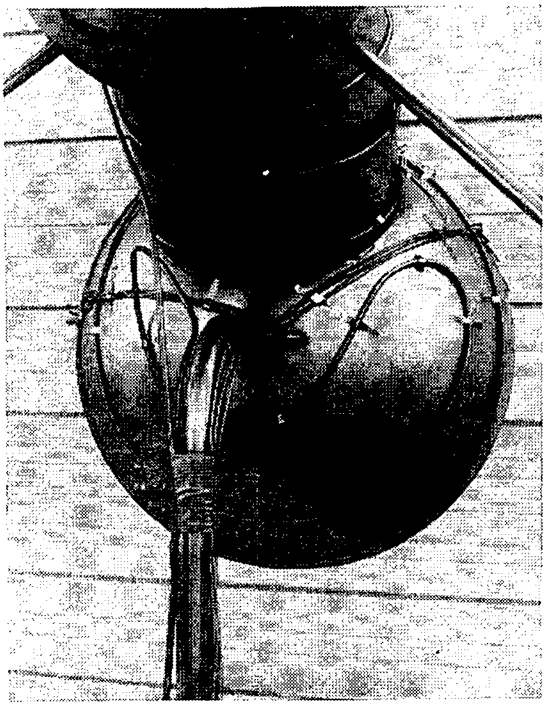

Figure 3. Photograph of preheaters on sodium pool-boiler receiver.

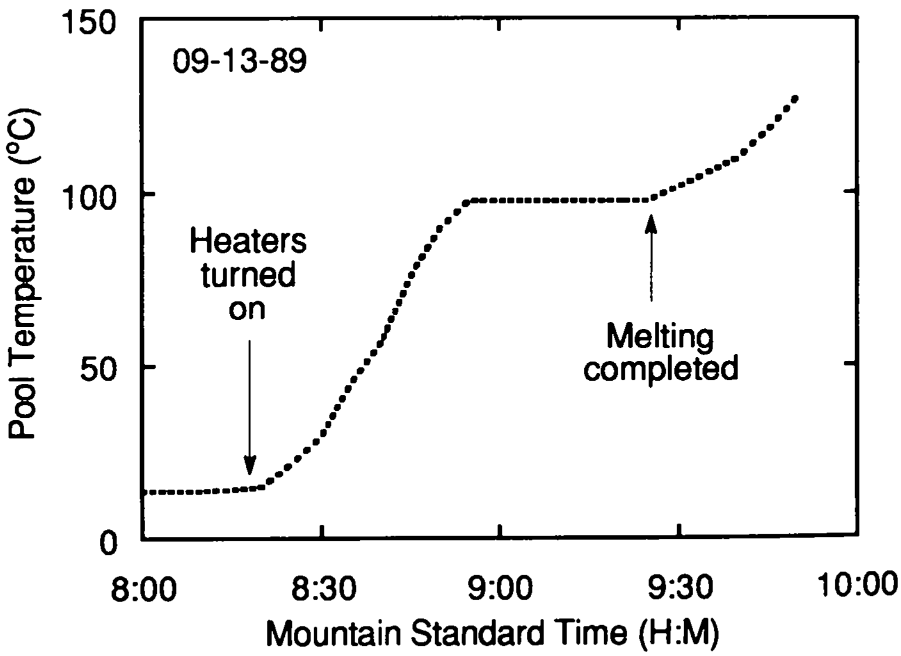

Figure 4. Temperature-time history during preheating to melt sodium in first full-scale pool boiler.

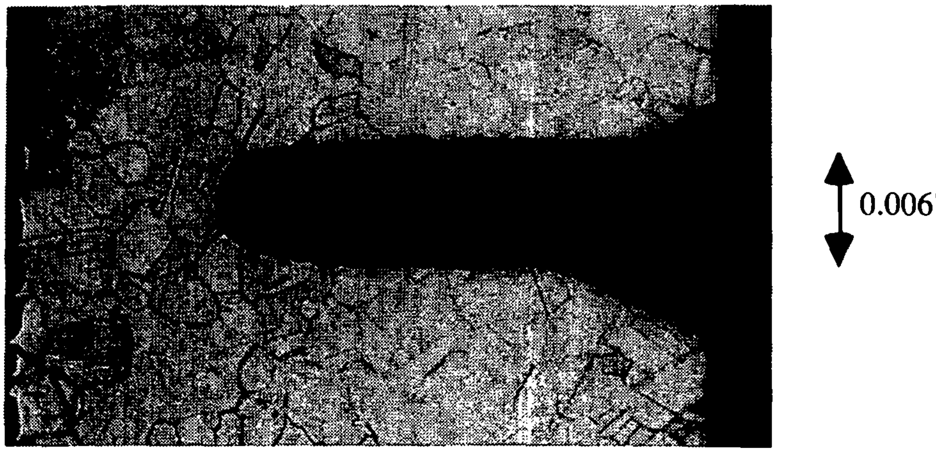

Figure 5. Cross section (post-test) of typical EDM cavity used in the sodium pool-boiler receiver.

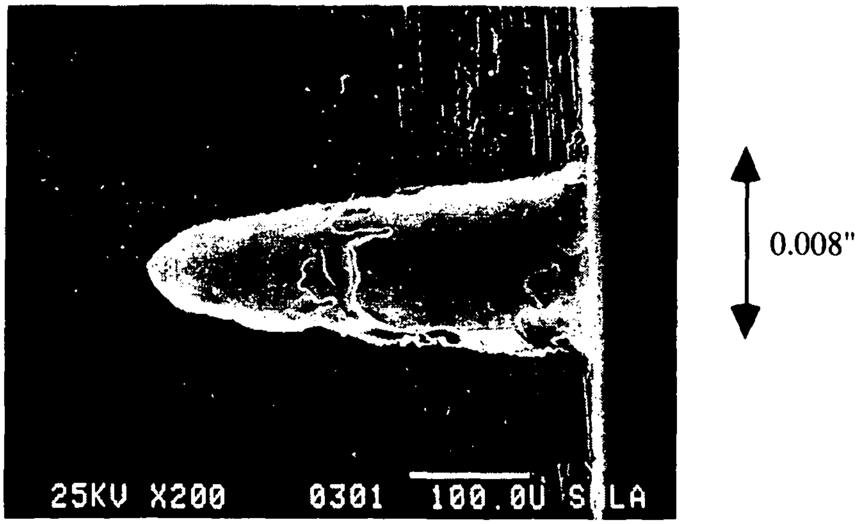

Figure 6. Cross section of laser-drilled cavity prototype for the present bench test.

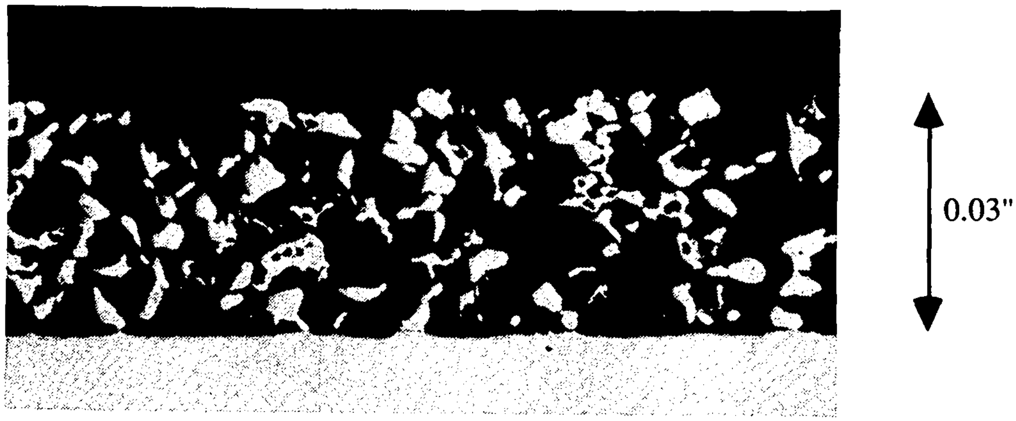

Figure 7. Cross section of hot-press-sintered powdered-metal patch prototype, present bench tests.

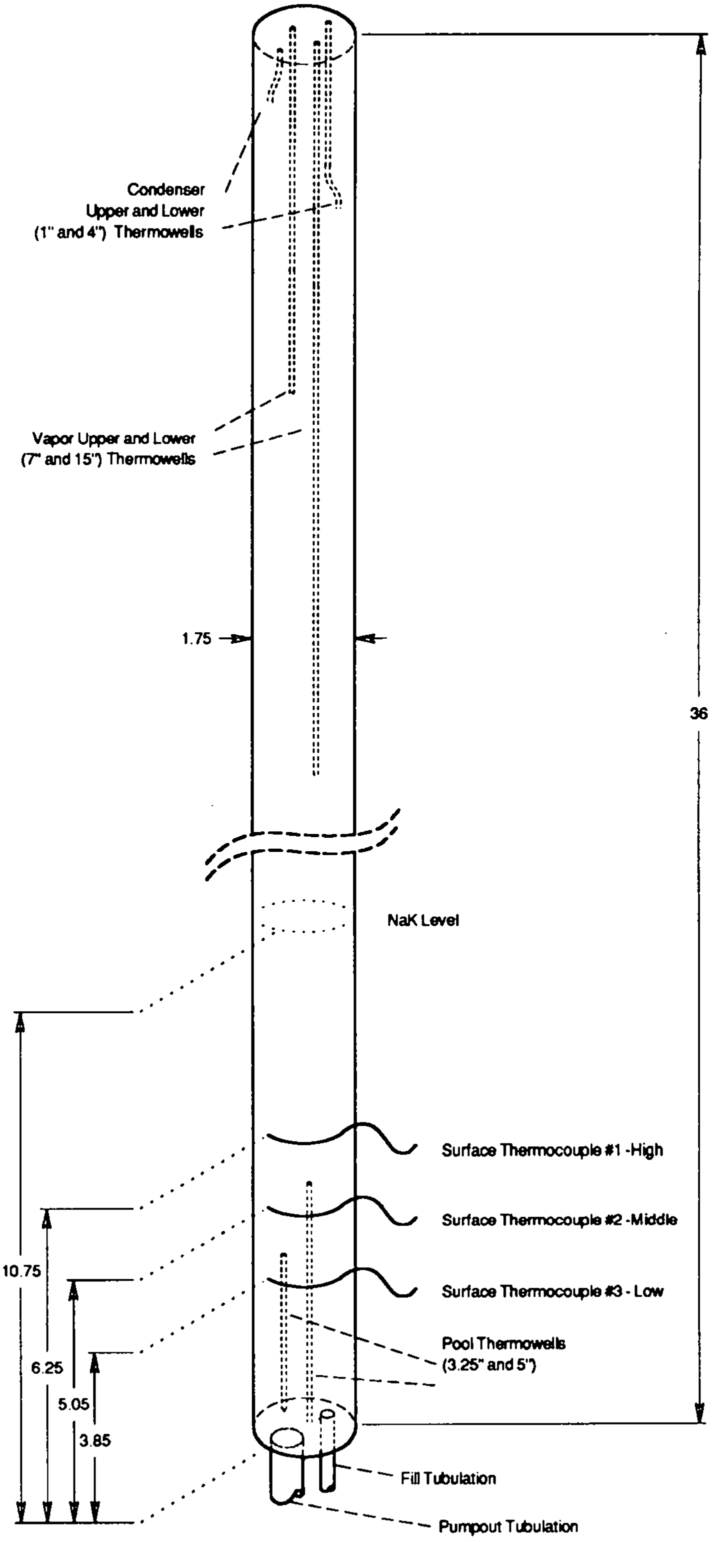

Figure 8. Bench-scale pool-boiler design (typical). Alternative surface thermocouple placements are shown in Figures 9 and 12.

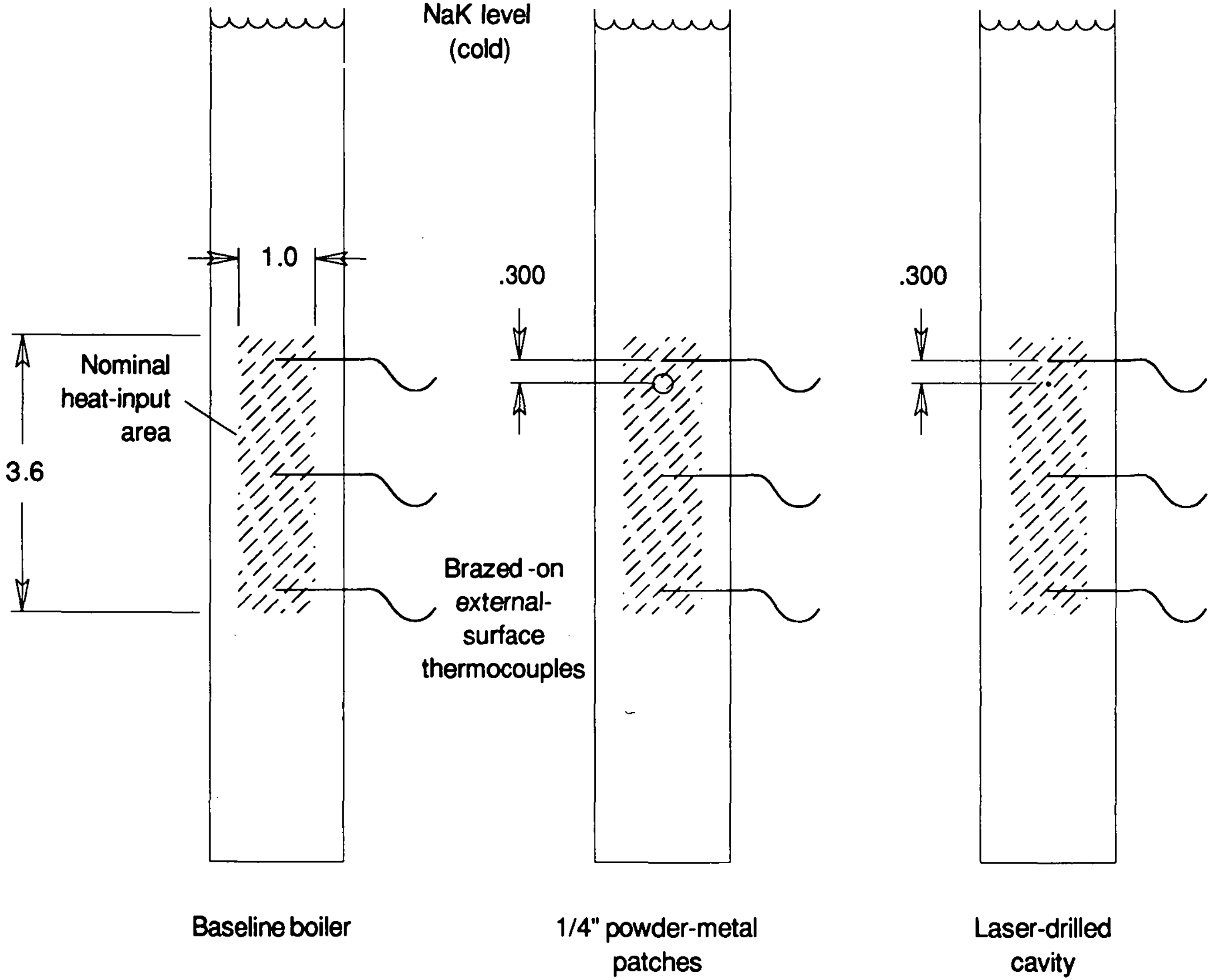

Figure 9. Placement of surface modifications in first four bench-scale boilers.

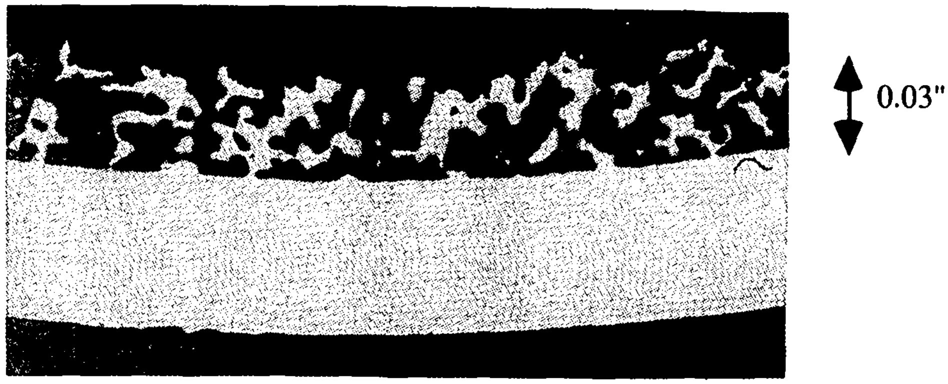

Figure 10. Cross section of -60/+80 stainless-steel powder coating prototype for the present bench test (applied by Friction Coating, Inc.).

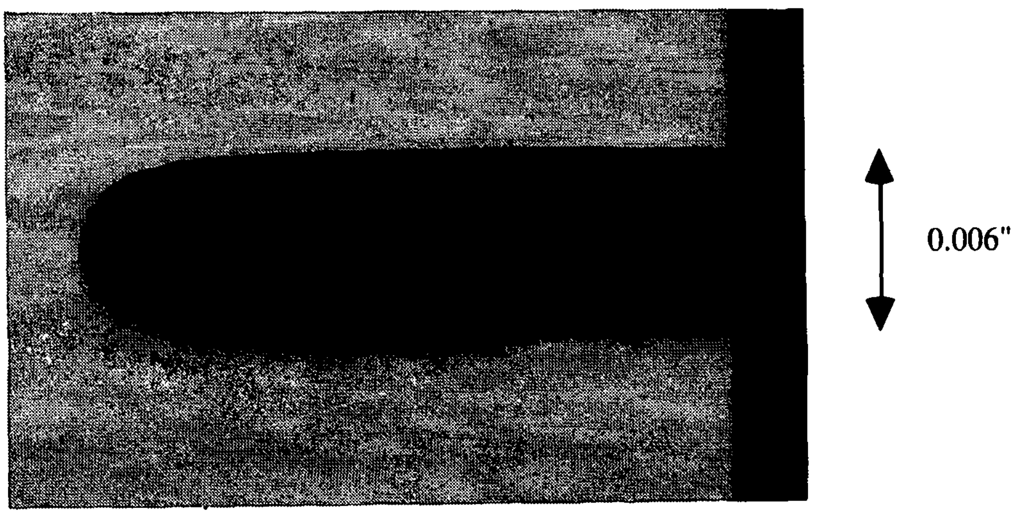

Figure 11. Cross section of EDM cavity prototype for the bench-scale boiler.

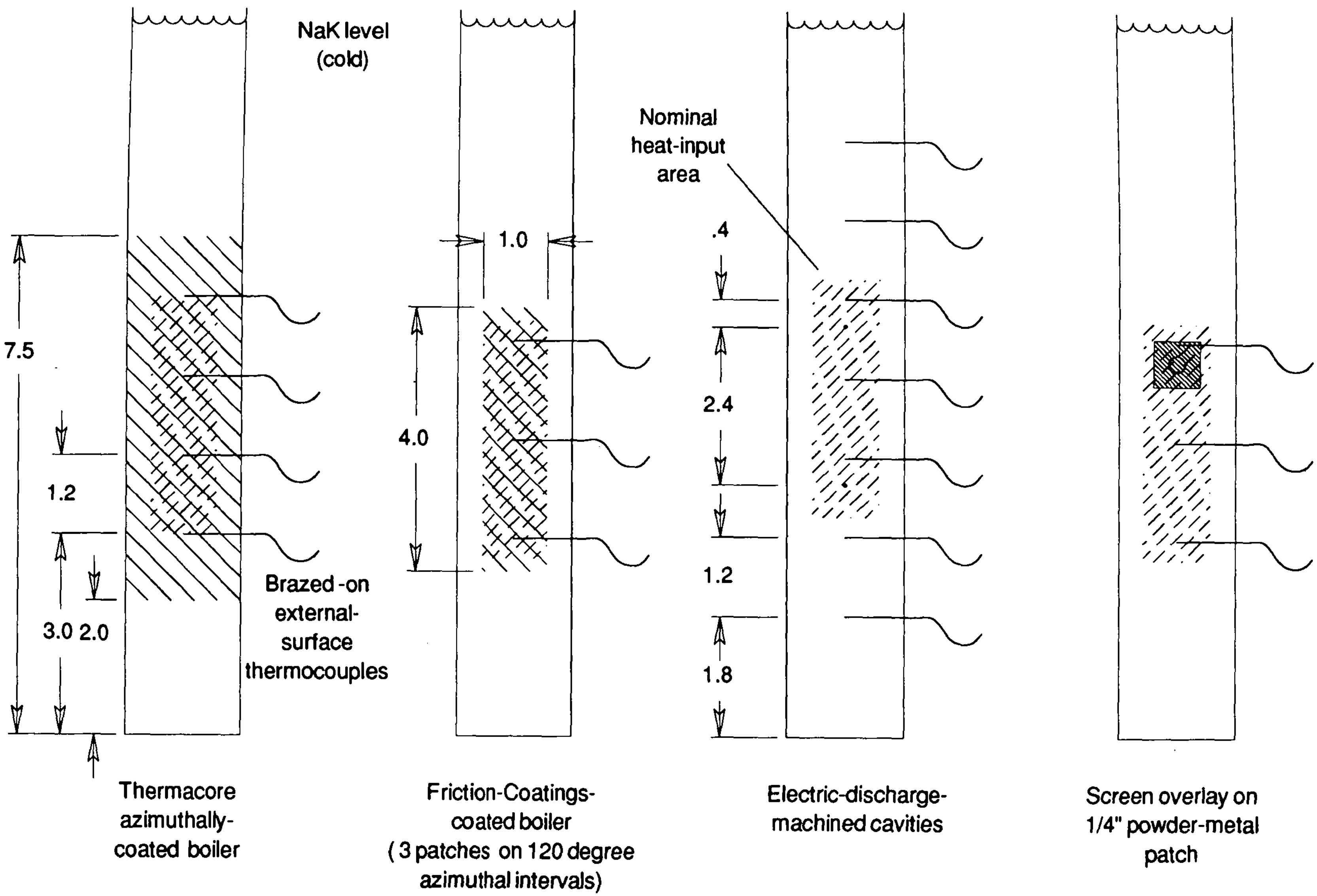

Figure 12. Placement of surface modifications in second four bench-scale boilers.

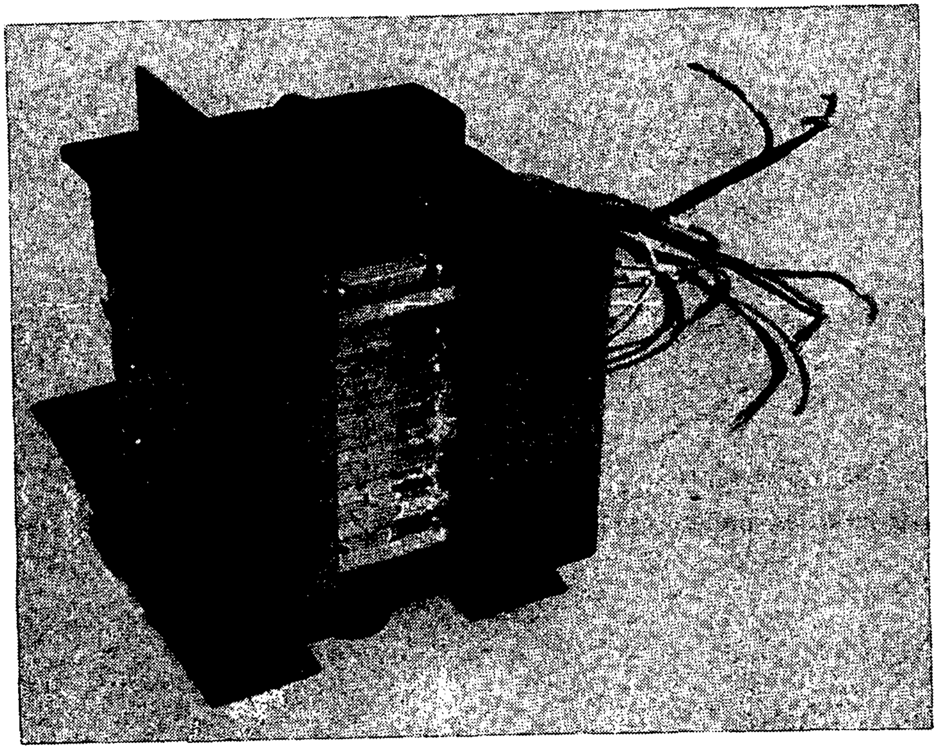

Figure 13. Quartz lamp assembly.

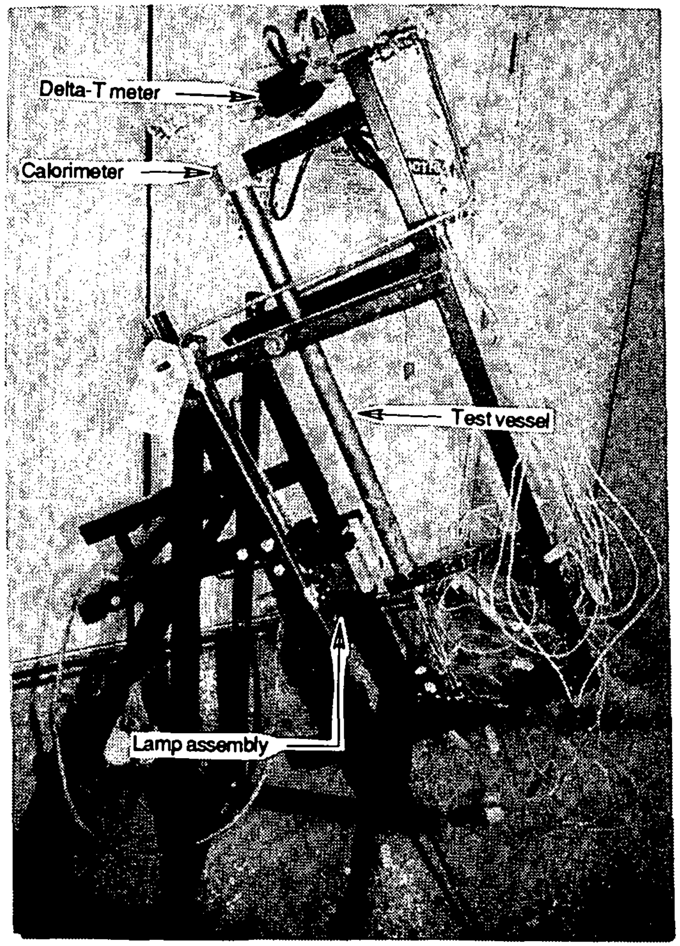

Figure 14. Rotatable test stand.

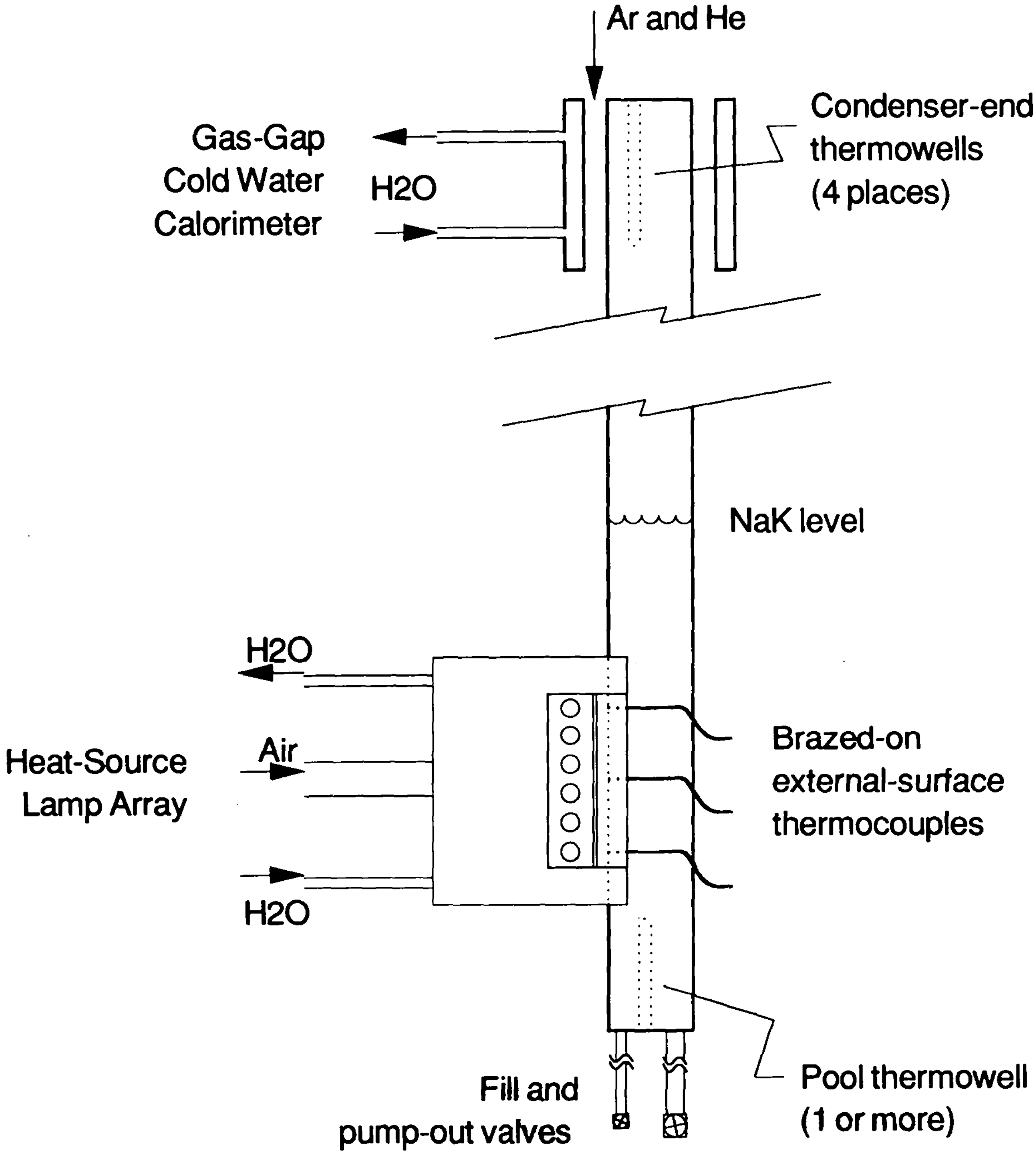

Figure 15. Schematic of bench-scale test apparatus.

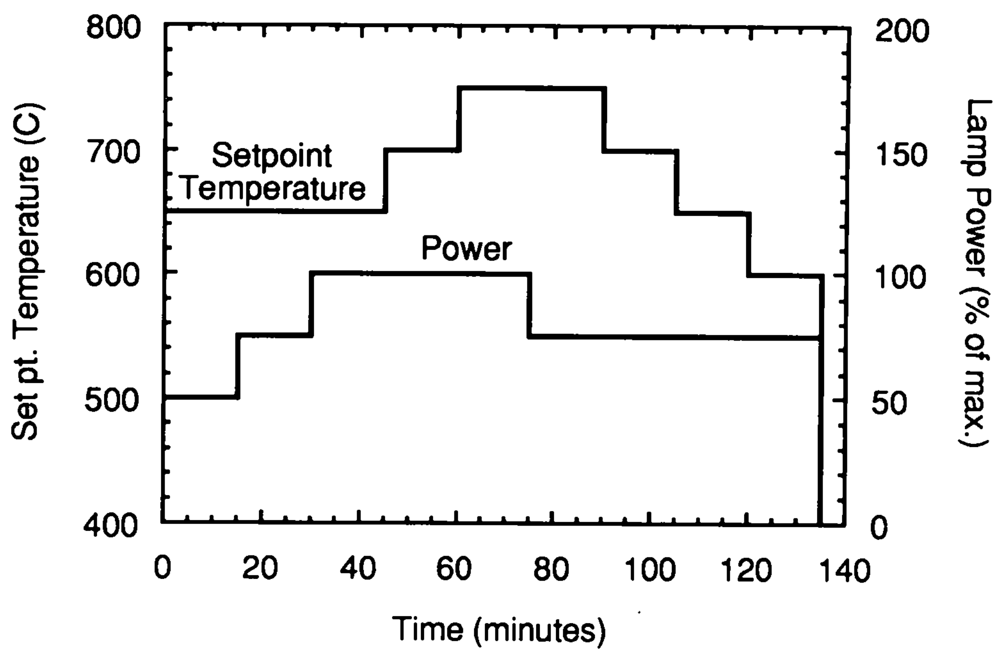

Figure 16. Boiling-stability test sequence; the controlled temperature (setpoint) was normally measured at the lower condenser thermocouple.

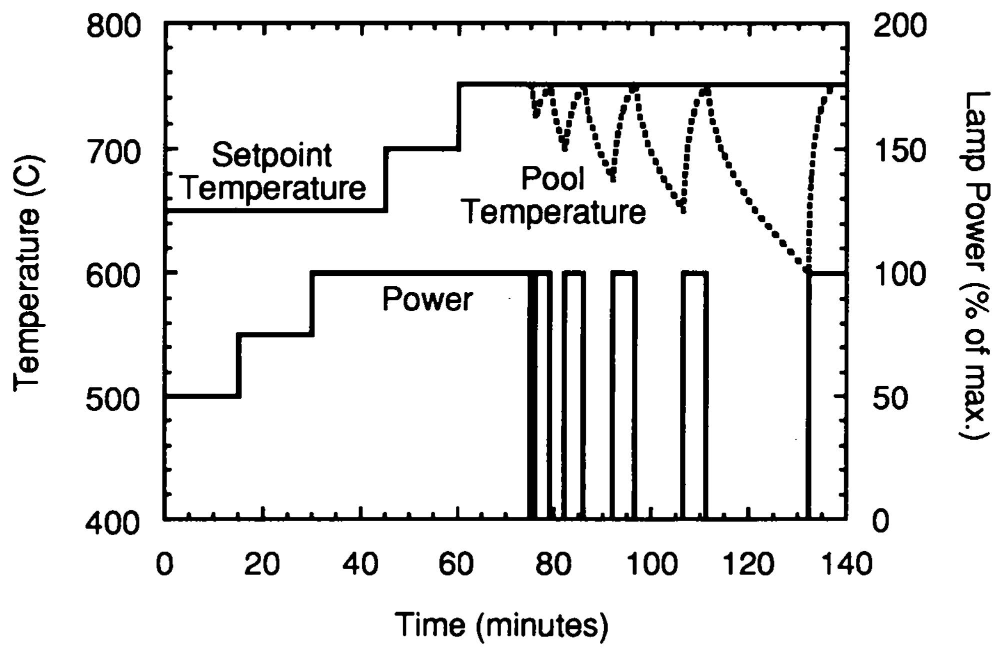

Figure 17. Sequence for hot-restart tests; the controlled temperature (setpoint) was normally measured at the lower condenser thermocouple.

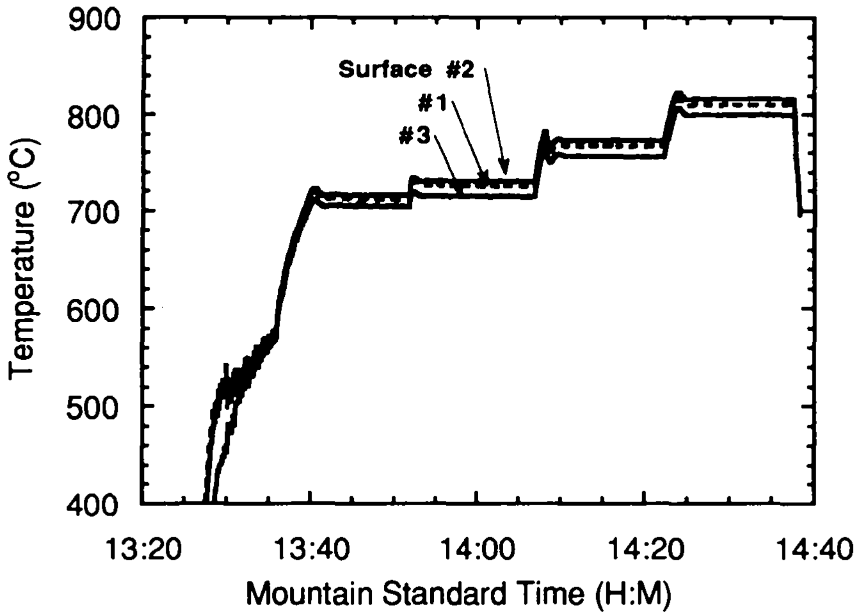

Figure 18. Heated-surface temperatures during a stable-boiling run; thermocouples are numbered as shown in Figure 8.

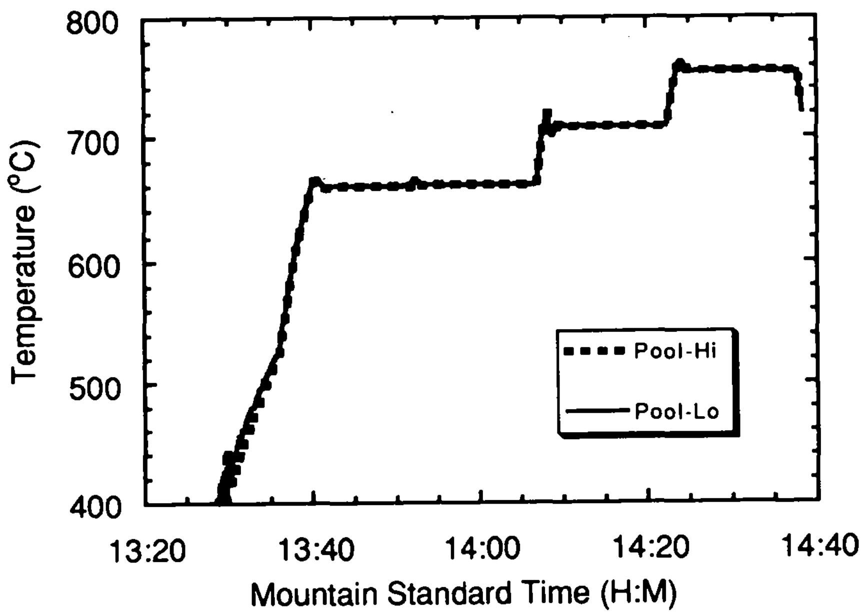

Figure 19. Pool temperatures during a stable-boiling run; see Figure 8 for thermocouple placement.

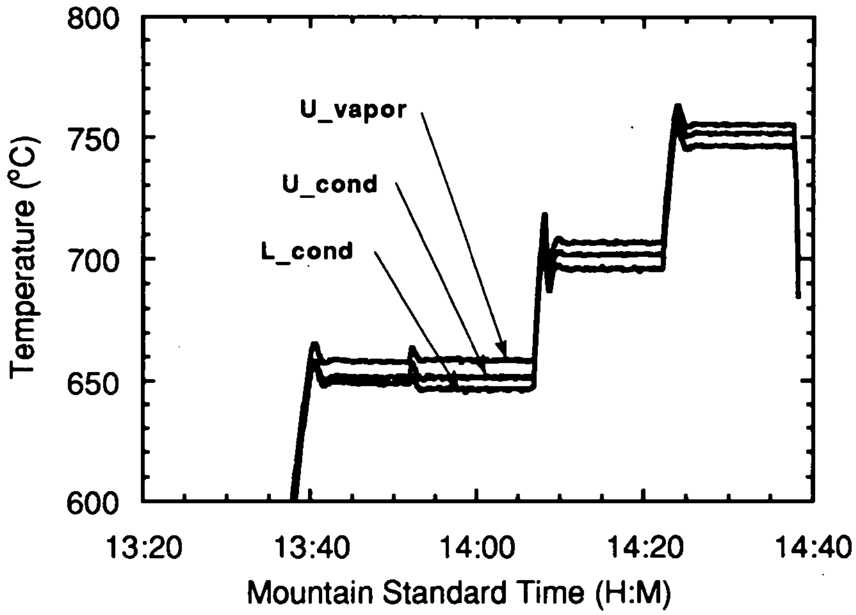

Figure 20. Vapor and condenser temperatures during a stable-boiling run; see Figure 8 for thermocouple placement (U_cond = upper condenser thermocouple, etc.).

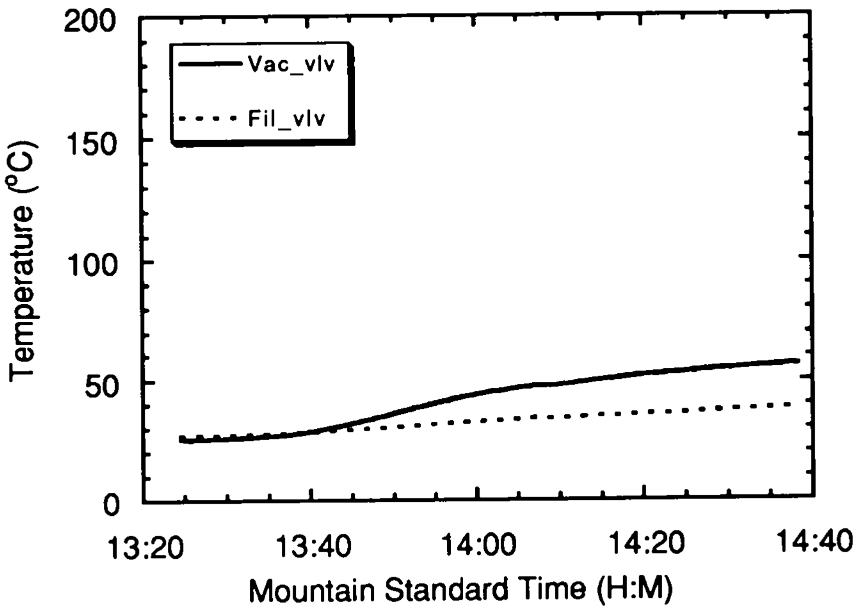

Figure 21. Boiler-valve (vacuum and fill) temperatures during a stable-boiling run.

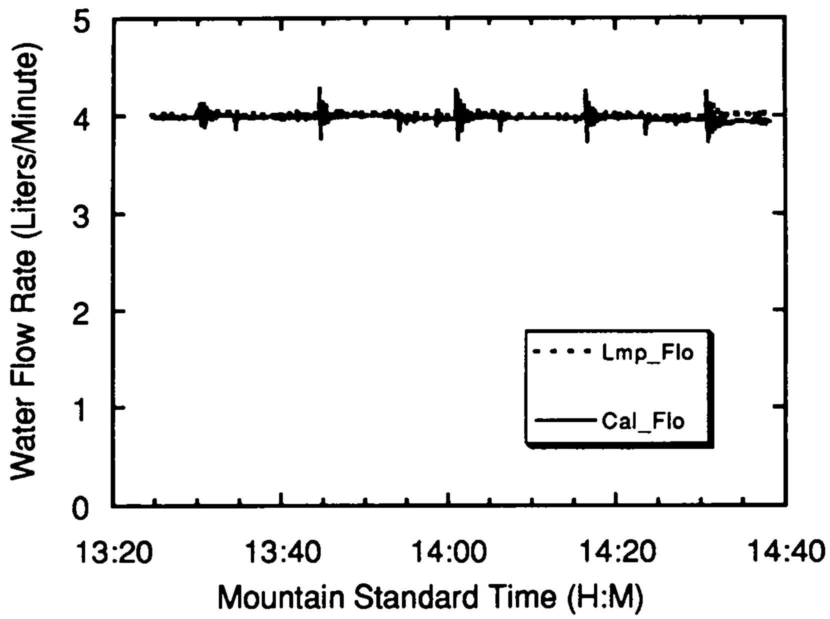

Figure 22. Water-flow rates through lamp assembly (Lmp_Flo) and calorimeter during a stable-boiling run.

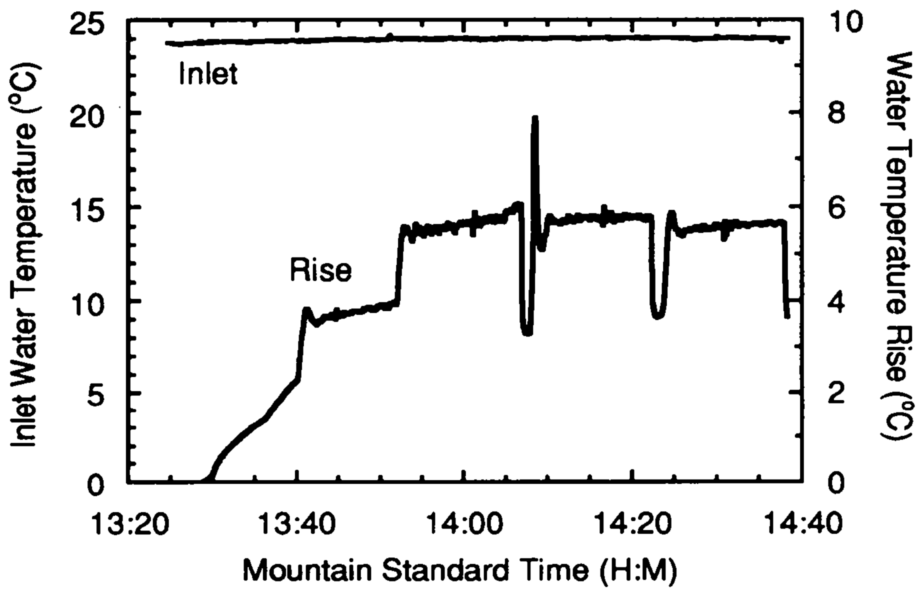

Figure 23. Calorimeter-water temperatures during a stable-boiling run.

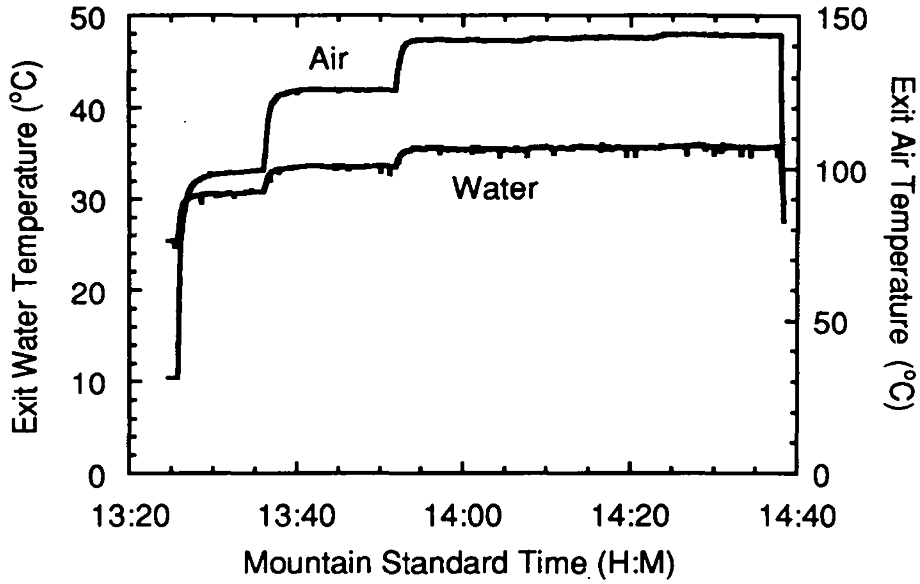

Figure 24. Lamp coolant exit temperatures during a stable-boiling run.

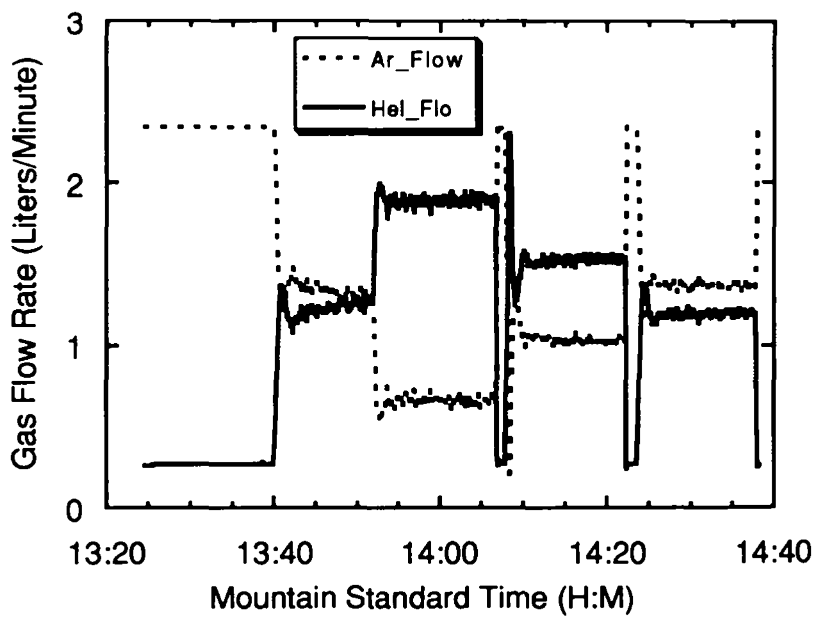

Figure 25. Calorimeter argon and helium flows during a stable-boiling run.

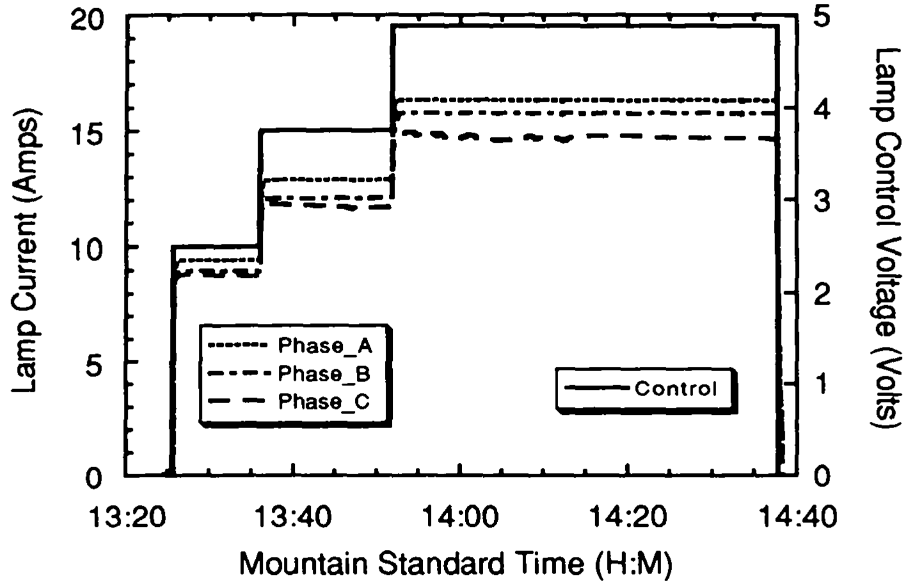

Figure 26. Lamp current and control voltage during a stable-boiling run.

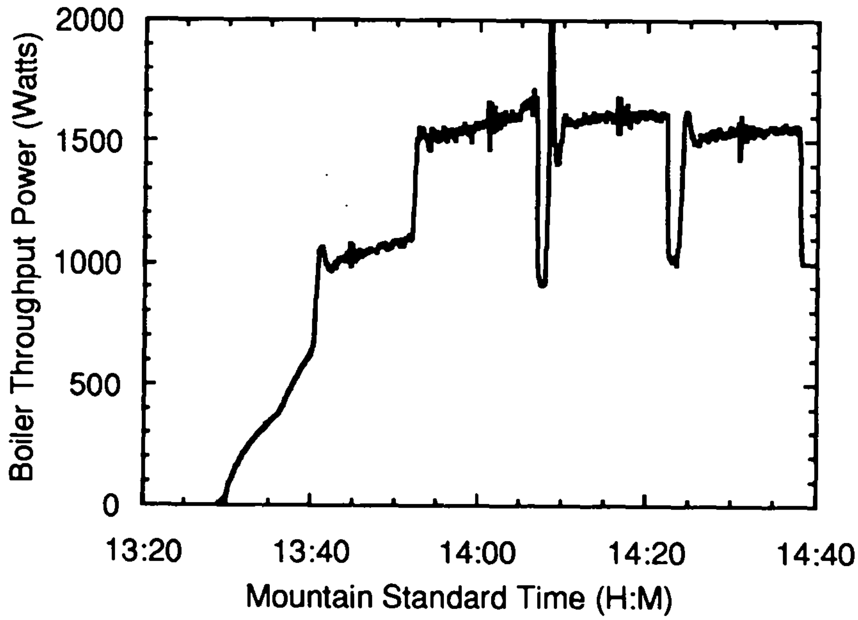

Figure 27. Boiler throughput power during a stable-boiling run.

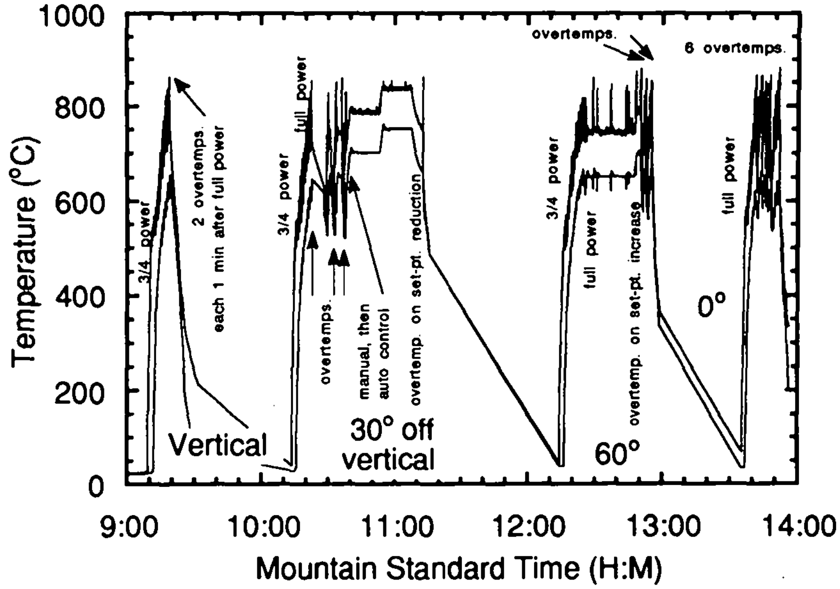

Figure 28. Boiling instability observed with the laser-drilled cavity; no added gas. In this and subsequent plots, the upper trace is a heated-surface temperature, and the lower trace is a condenser temperature. Notations indicate where various events occurred, such as changes in lamp power, or safety shutdowns caused by high temperatures (overtemperatures).

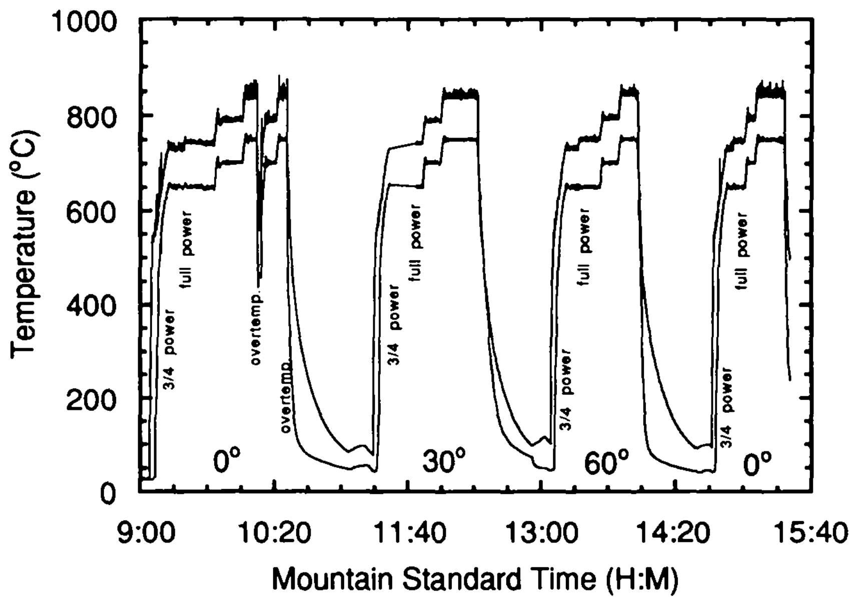

Figure 29. Improved stability with 1.5 torr of xenon (compare with Figure 28.)

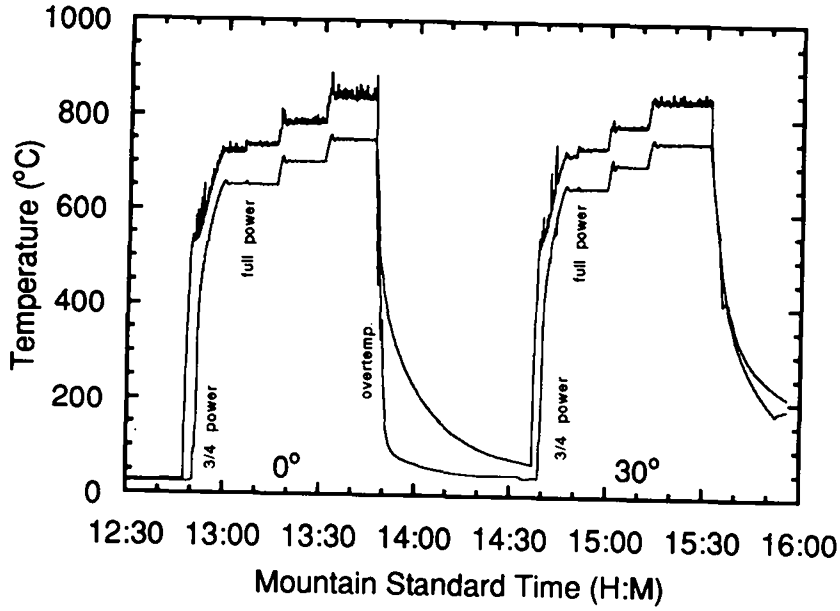

Figure 30. Stability improvement with 0.37 torr of xenon (compare with Figure 28).

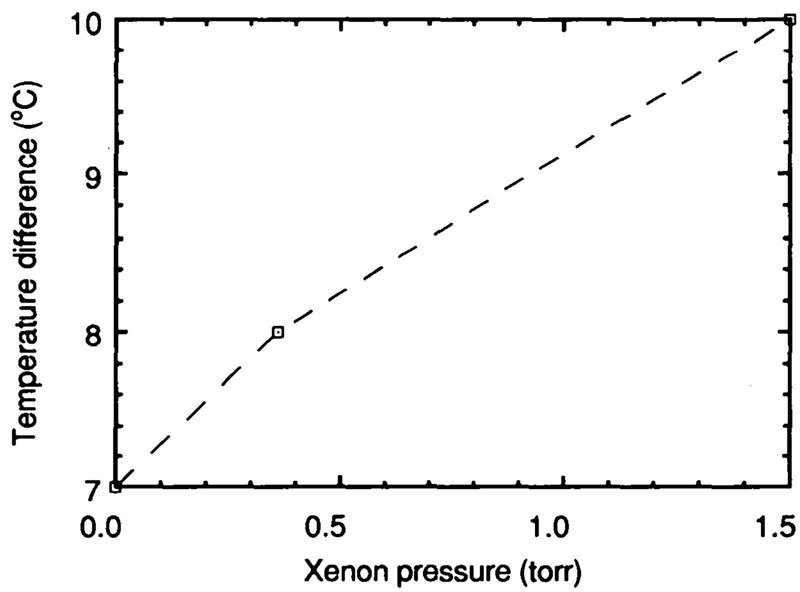

Figure 31. Effect of xenon pressure on pool to lower-condenser temperature difference.

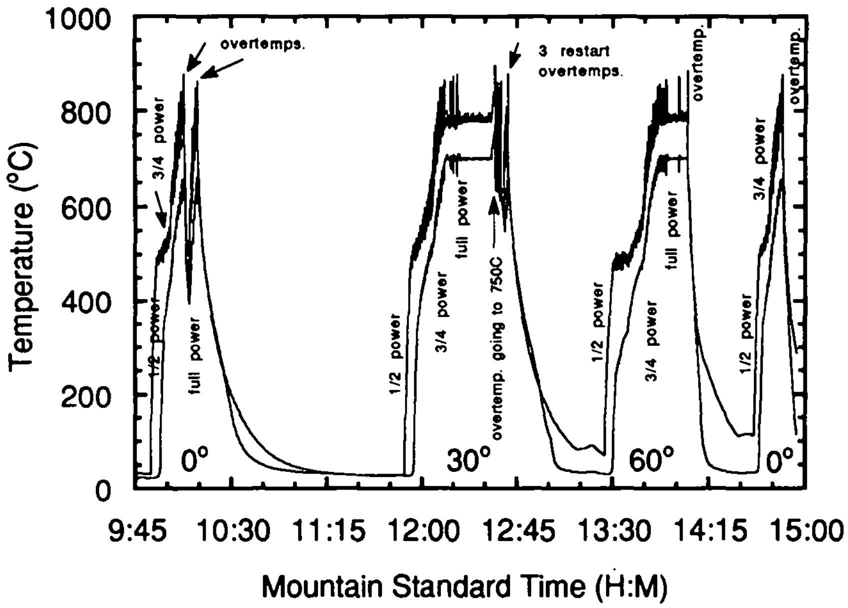

Figure 32. Boiling instability observed with the 1/4"-diameter IN600 coating; no added gas.

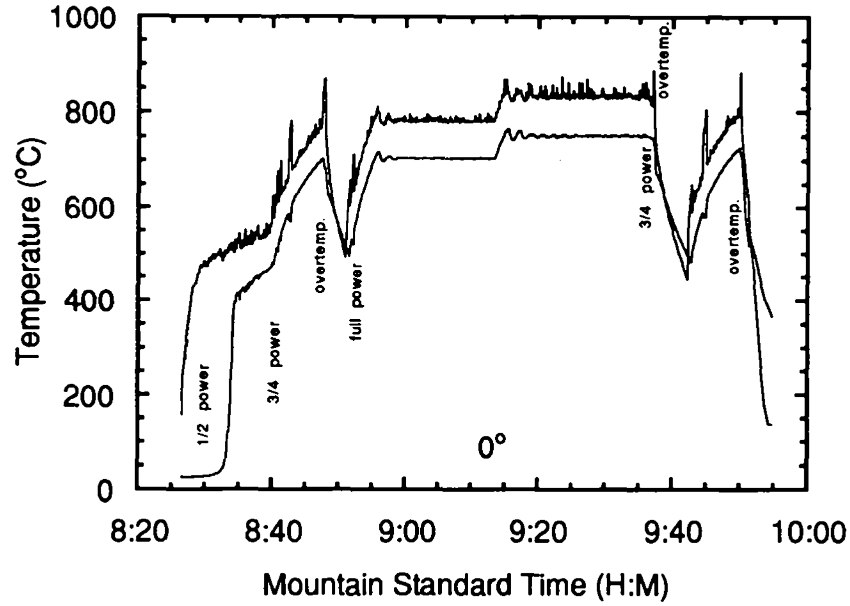

Figure 33. Stability improvement with 0.37 torr of xenon (compare with Figure 32).

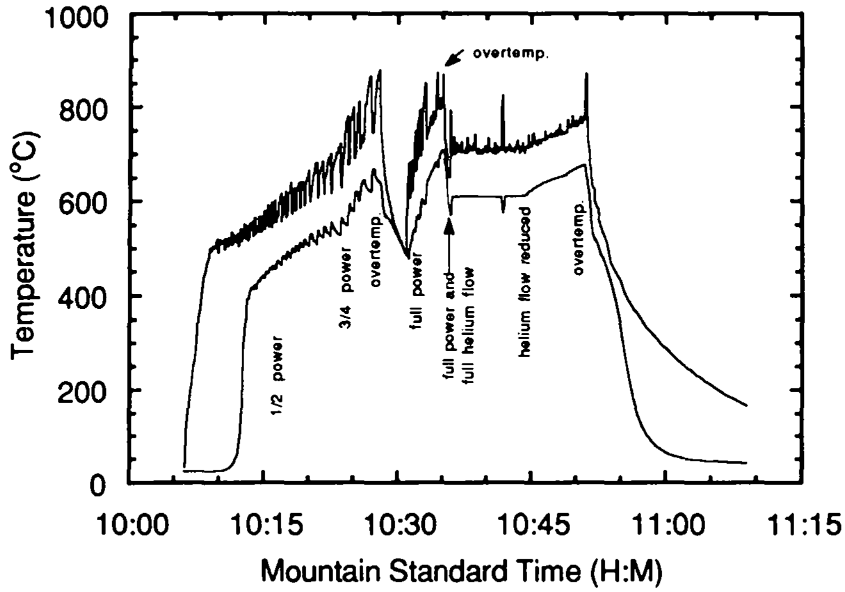

Figure 34. Less-stable behavior with 0.37 torr of *helium* (compare with Figures 32 and 33).

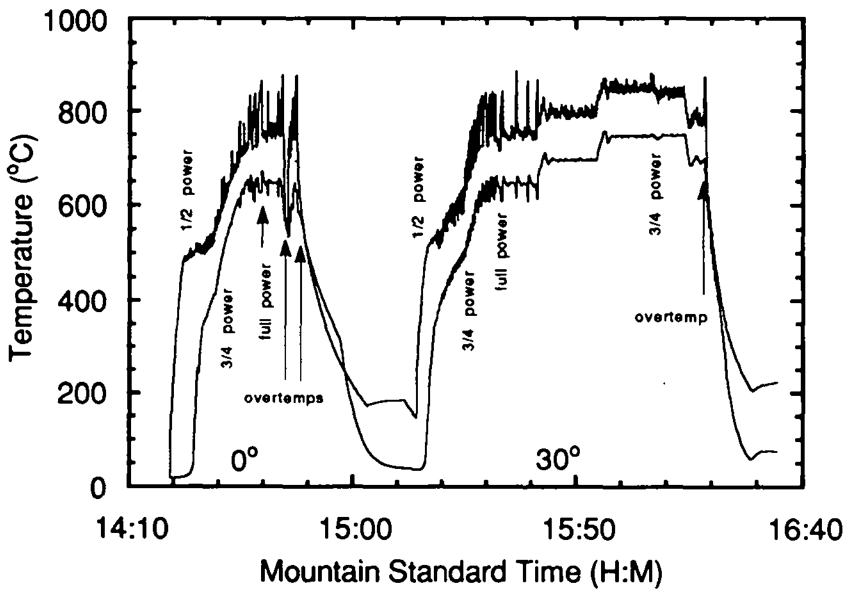

Figure 35. Boiling instability observed with the 1/4"-diameter 304L SS coating; no added gas.

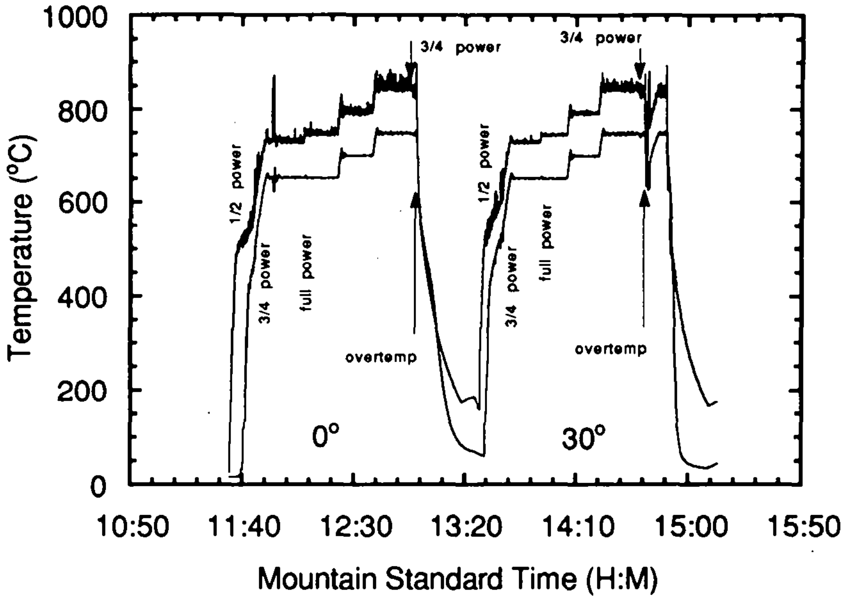

Figure 36. Stability improvement with 0.37 torr of xenon (compare with Figure 35).

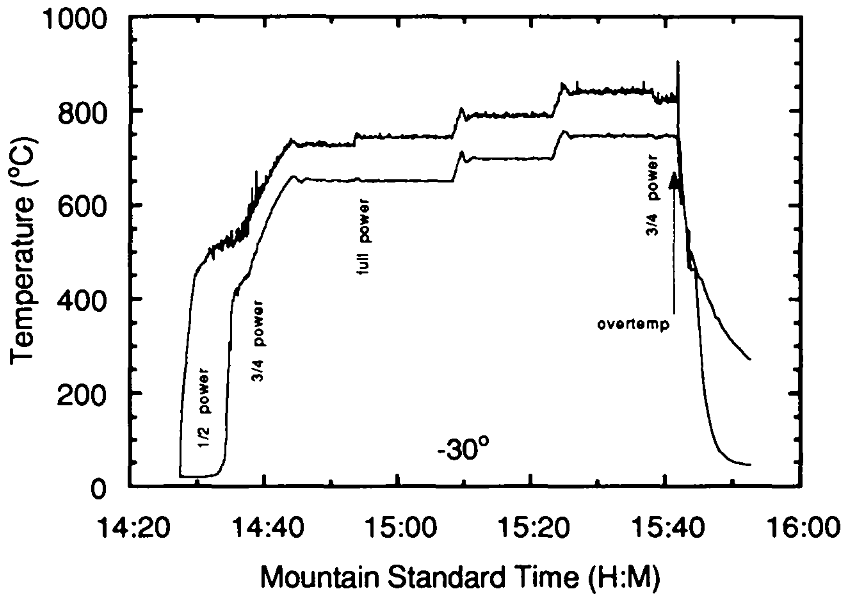

Figure 37. Effect of negative tilt for the 304L SS coating with 0.37 torr of xenon (compare with Figure 36).

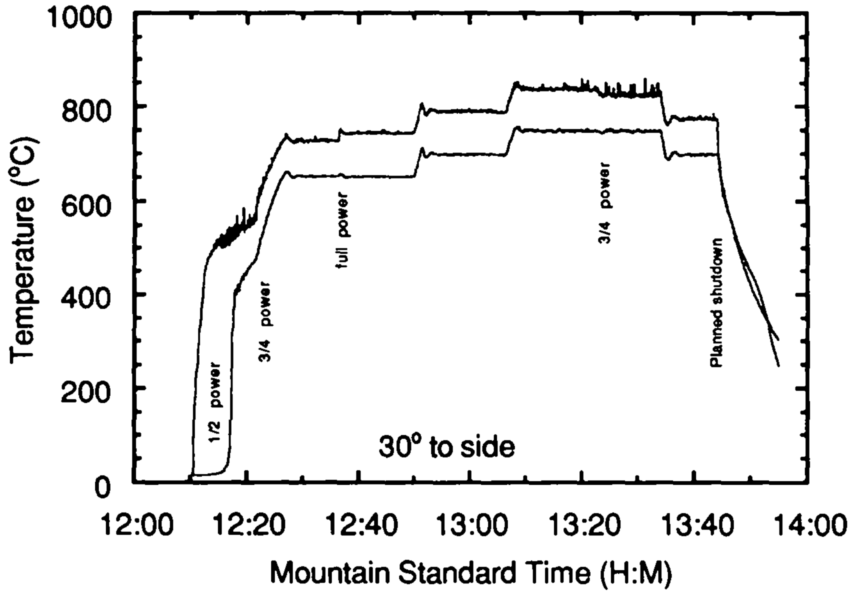

Figure 38. Effect of sideways tilt for the 304L SS coating with 0.37 torr of xenon (compare with Figures 36 and 37).

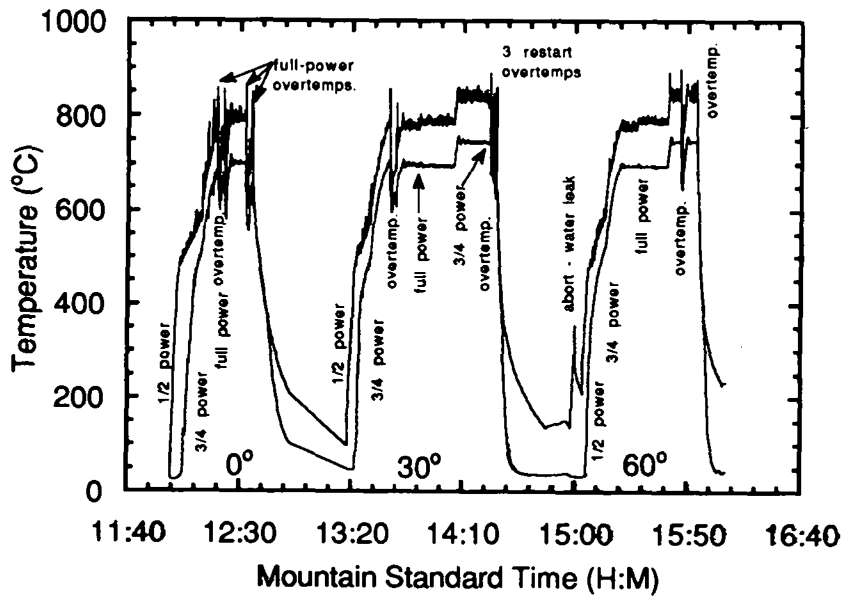

Figure 39. Boiling instability observed with the baseline boiler; no added gas.

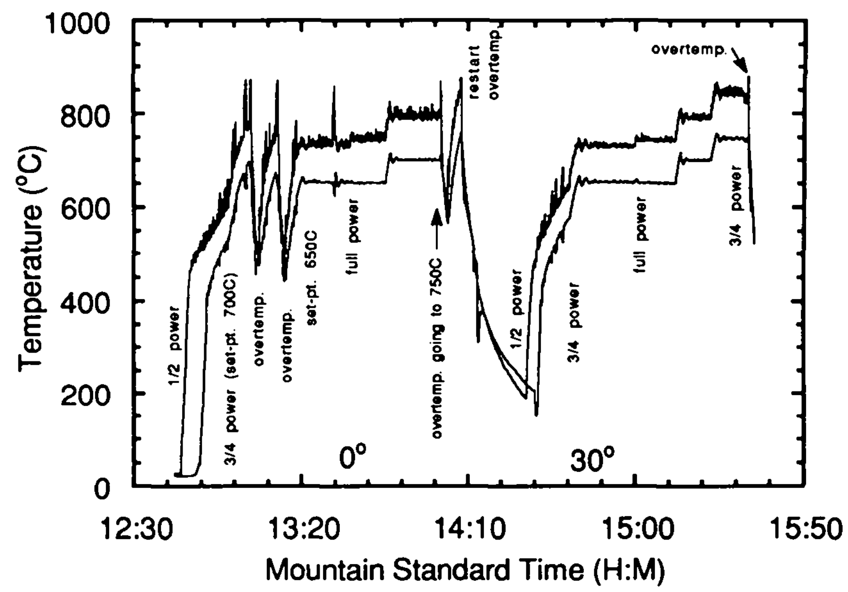

Figure 40. Stability improvement with 0.37 torr of xenon (compare with Figure 39).

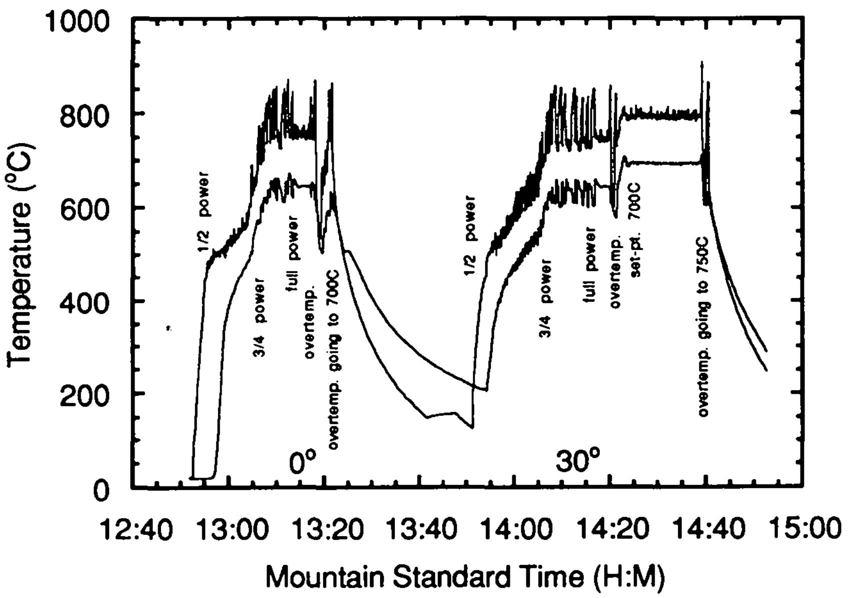

Figure 41. Instability observed with 50 ppm of O_2/no xenon (compare with Figures 39 and 40).

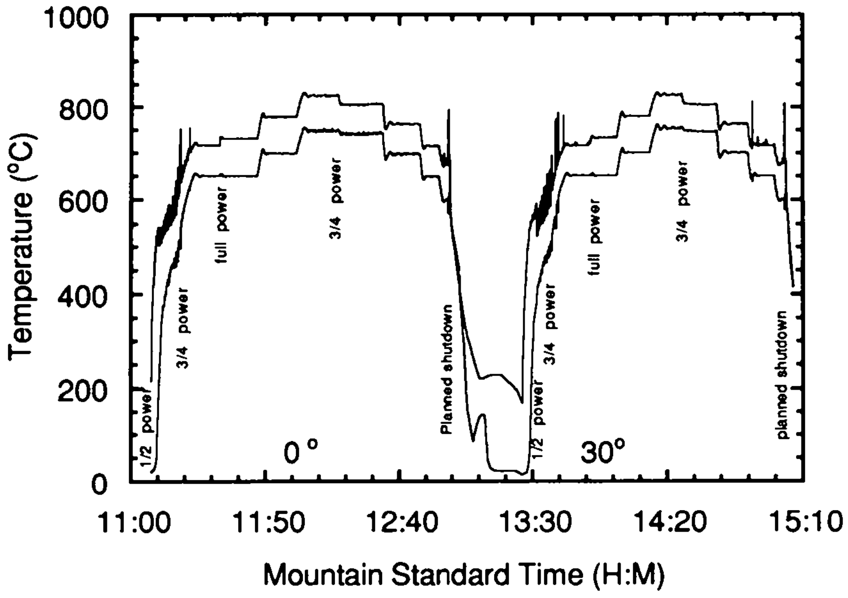

Figure 42. Stability observed with the Thermacore coating; no added gas.

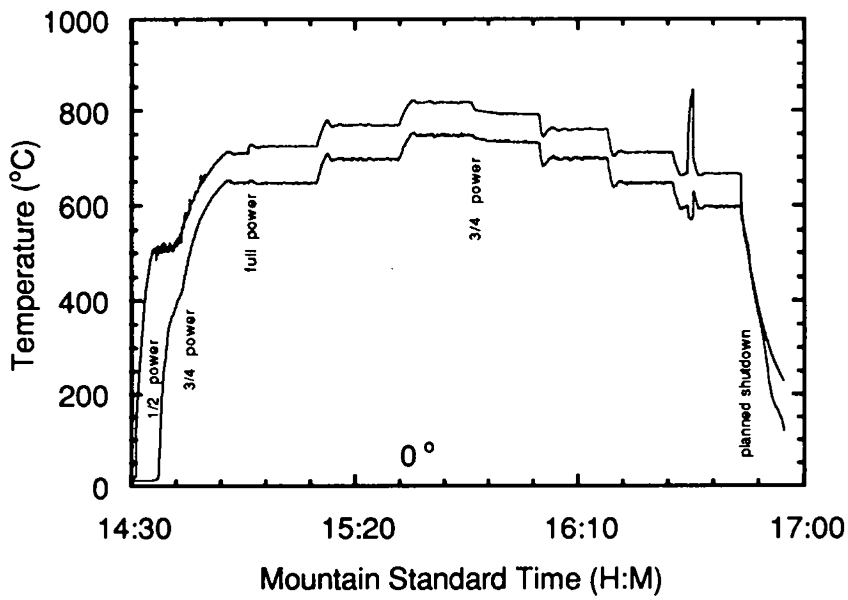

Figure 43. Stability observed with the -80/+100 Friction Coatings powder; no added gas.

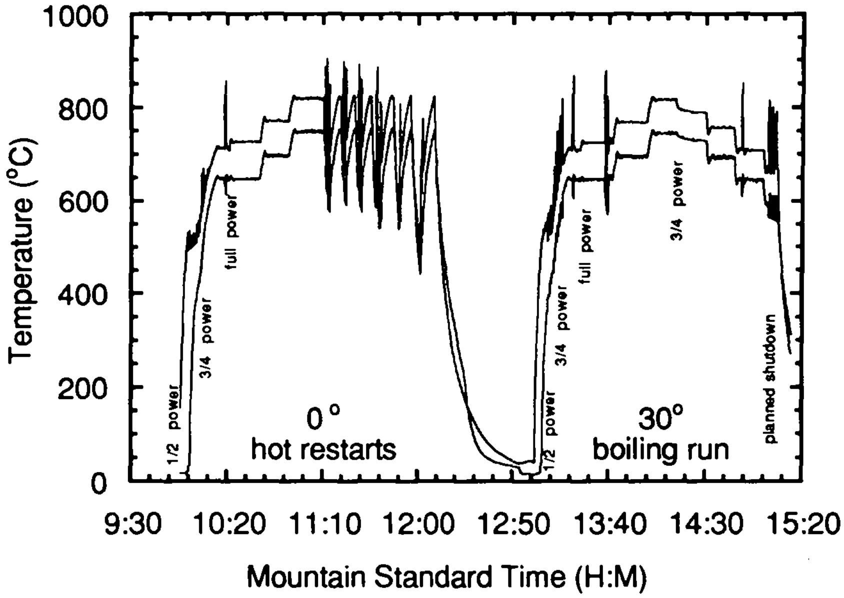

Figure 44. Boiling and hot restarts with the -80/+100 Friction Coatings powder; no added gas.

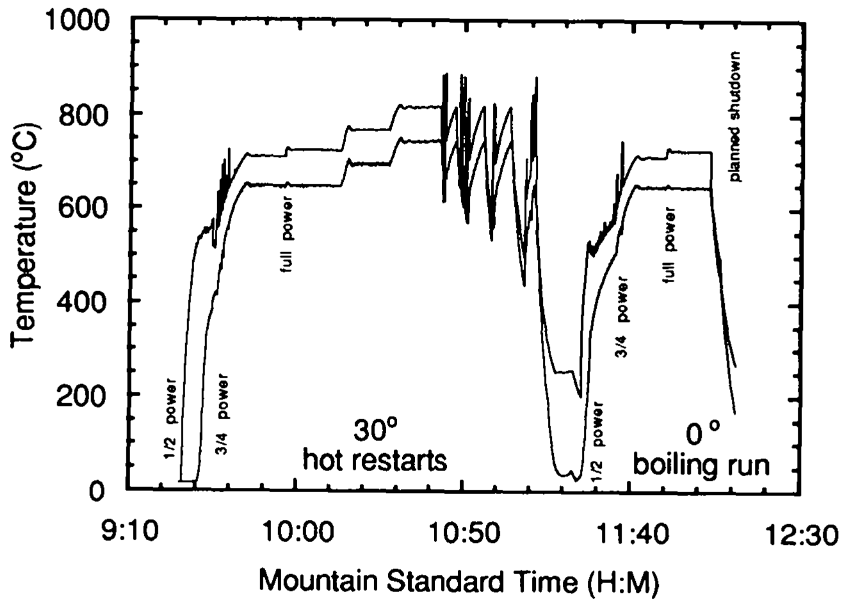

Figure 45. Boiling and hot restarts with the -80/+100 Friction Coatings powder; no added gas.

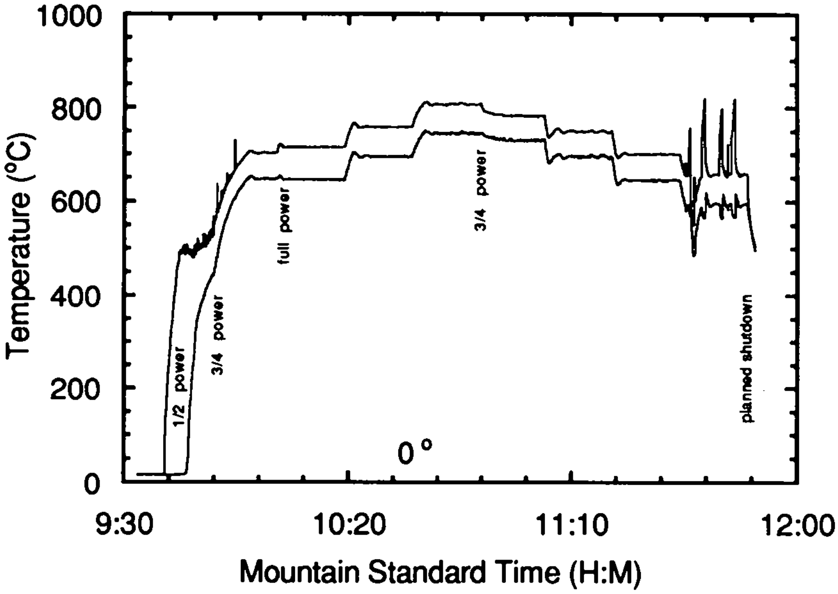

Figure 46. Repeat of test shown in Figure 43 illustrating random nature of boiling cessation.

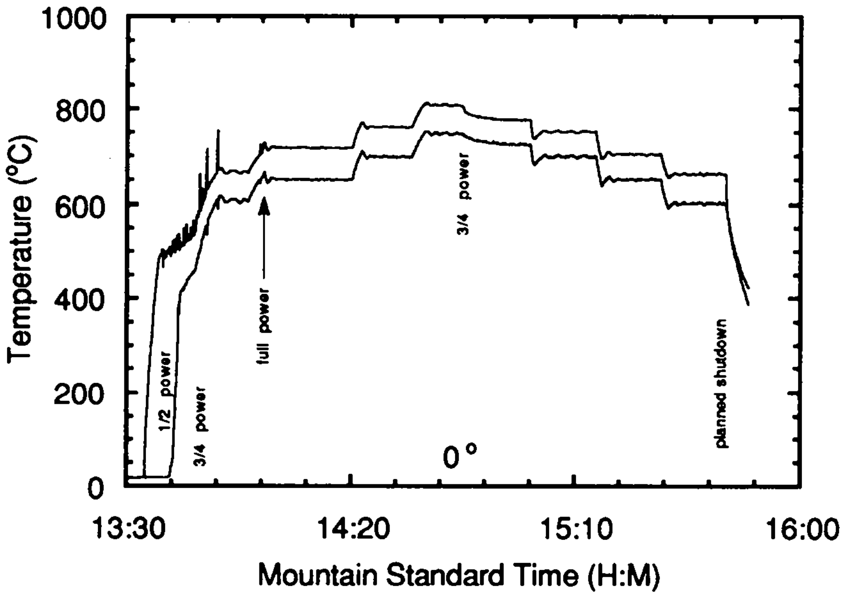

Figure 47. Improved stability with 0.37 torr of xenon (compare with Figures 43-46).

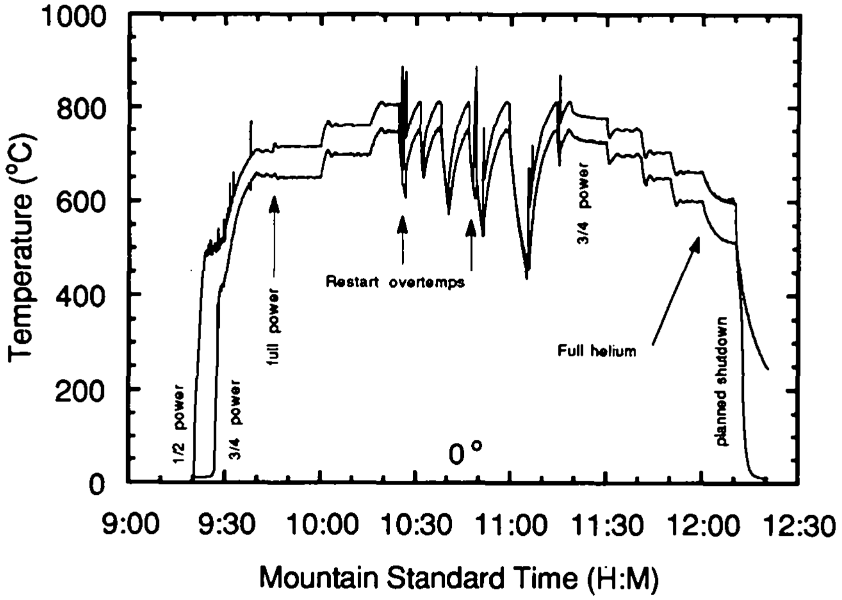

Figure 48. Improved hot restarts with 0.37 torr of xenon (compare with Figure 44).

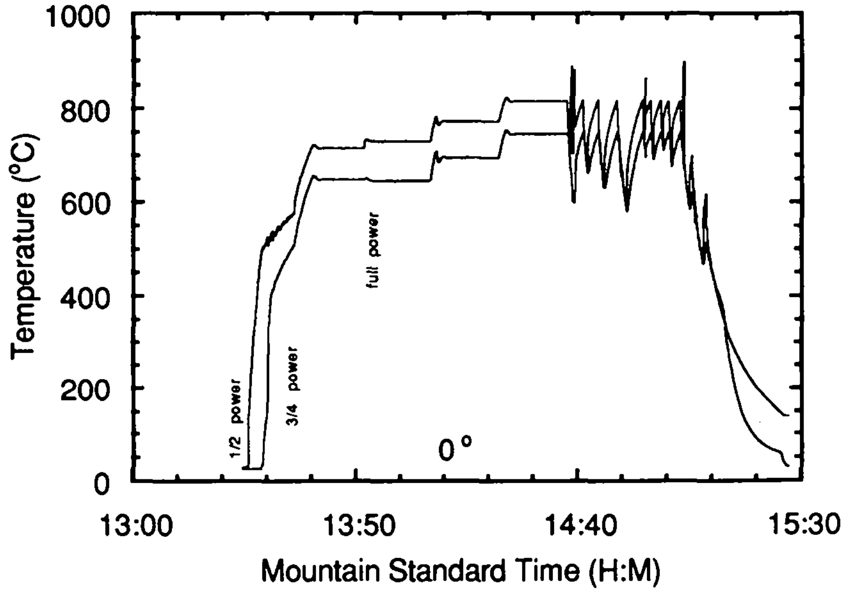

Figure 49. Improved hot restarts with boiler described in Figure 48 shortened to 24" (no safety-system shutdowns, lower percentage of temperature spikes).

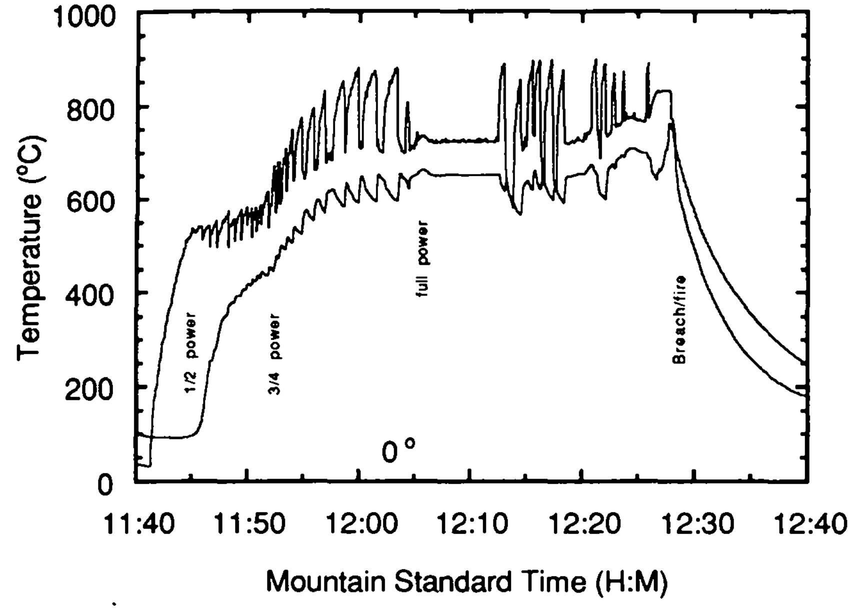

Figure 50. Boiling instability observed EDM cavities; no added gas.

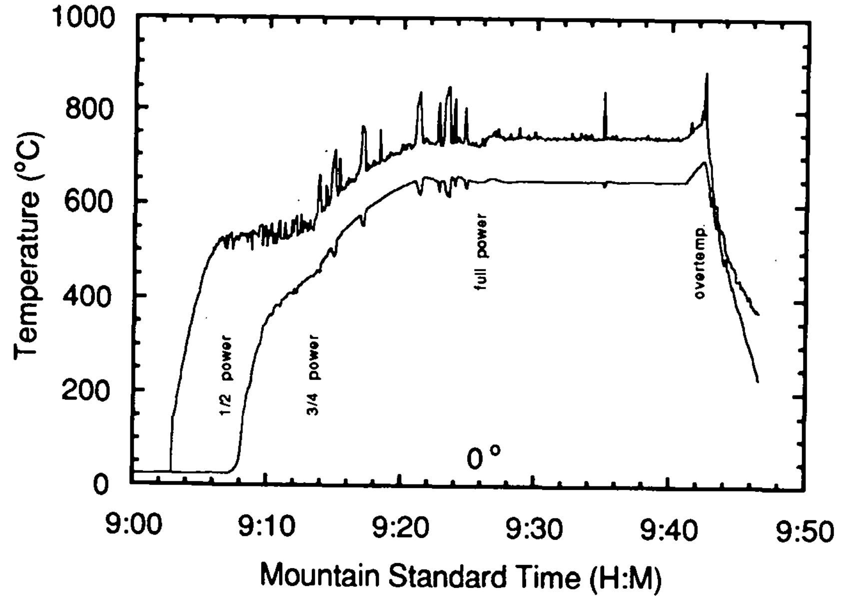

Figure 51. Improved stability after overlaying 1/4"-diameter IN600 coating with screen; no added gas (compare with Figure 32).

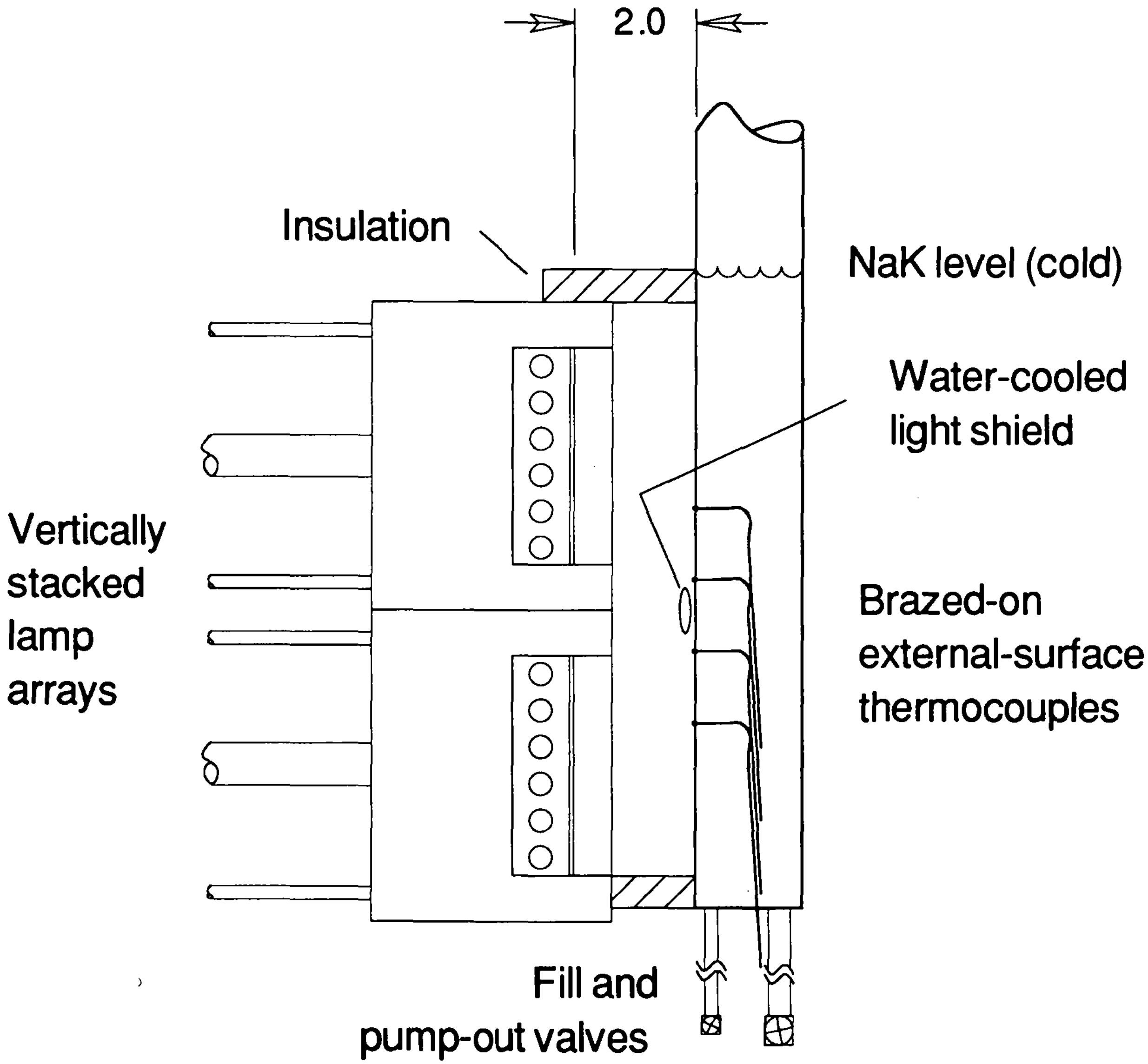

Figure 52. Arrangement of vertically-stacked lamps next to boiler. Light shield was a flattened tube shown here in cross section, through which cooling water flowed.

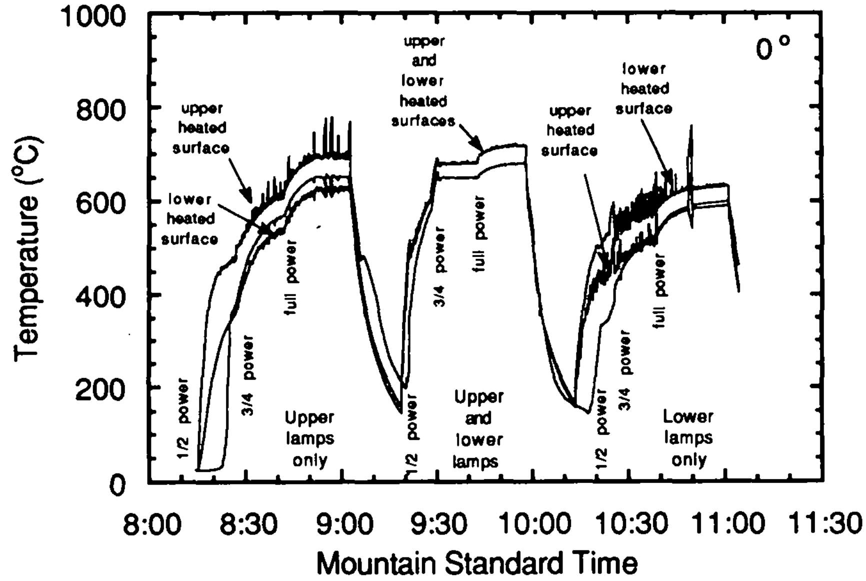

Figure 53. Boiling runs with vertically-stacked lamps and Thermacore coating; no added gas.

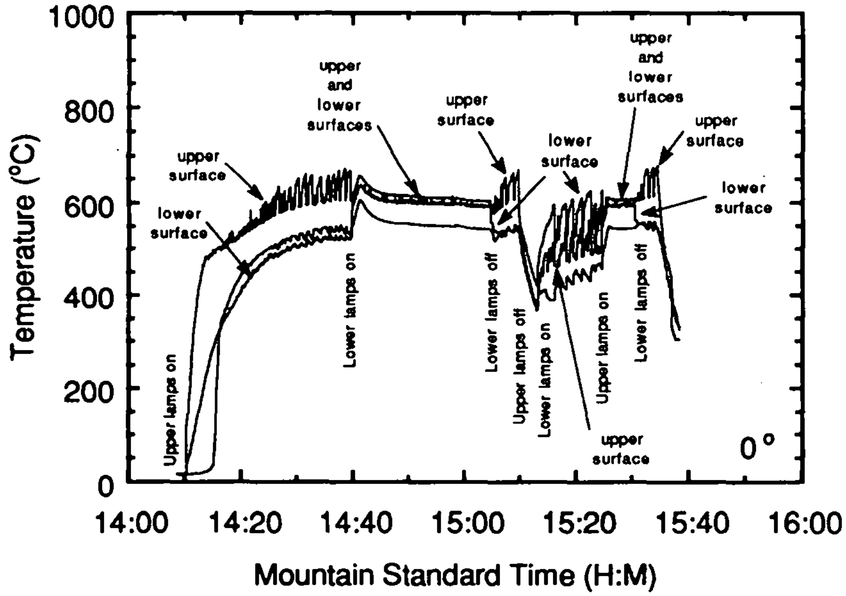

Figure 54. Boiling runs with stacked lamps, light shield and Thermacore coating; no added gas.

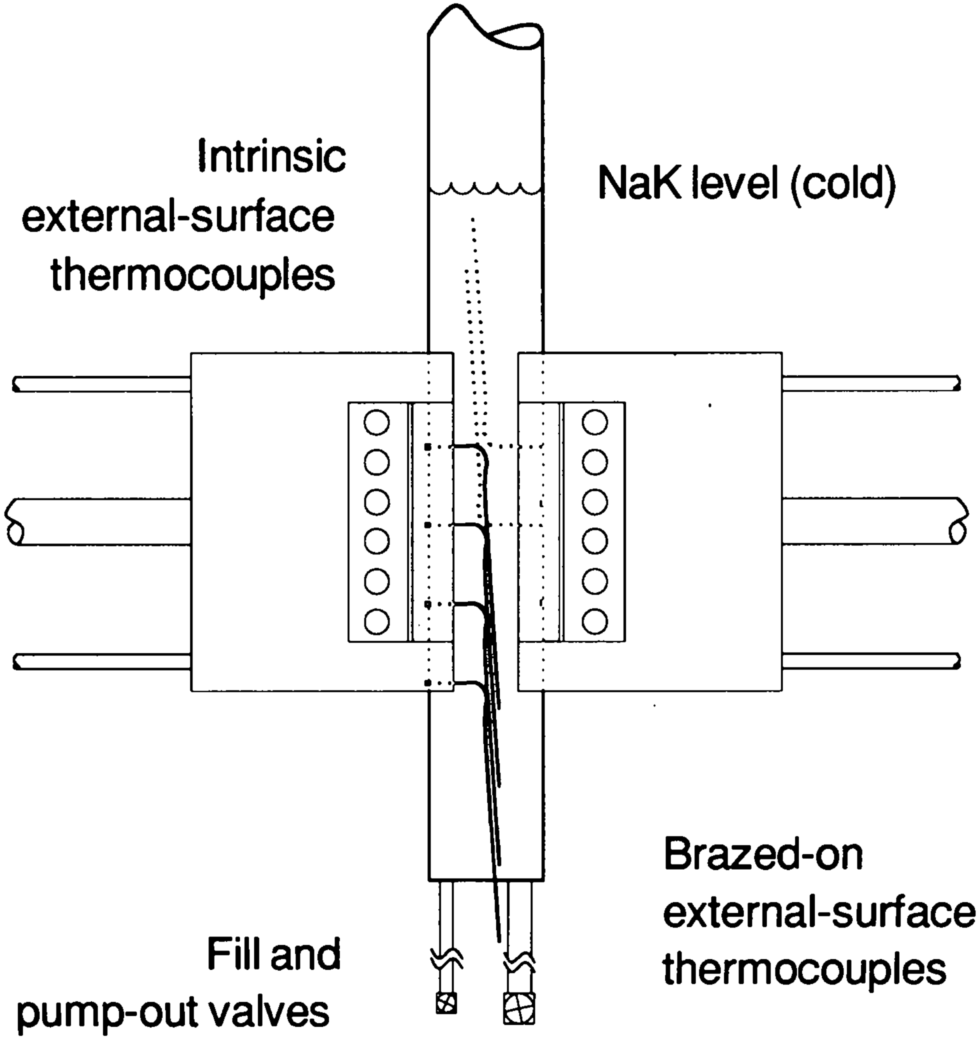

Figure 55. Arrangement of lamps on opposite sides of boiler.

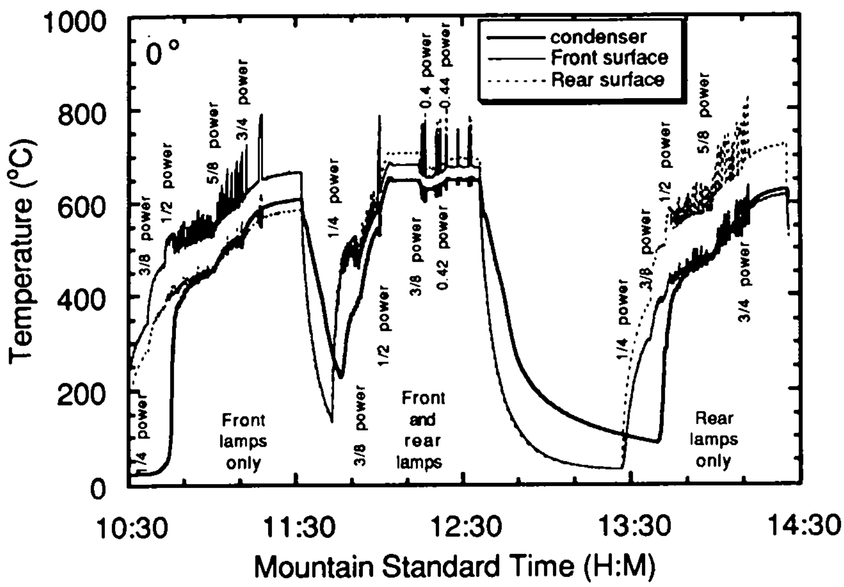

Figure 56. Boiling runs with lamps on opposite sides of Thermacore-coated boiler; no added gas.

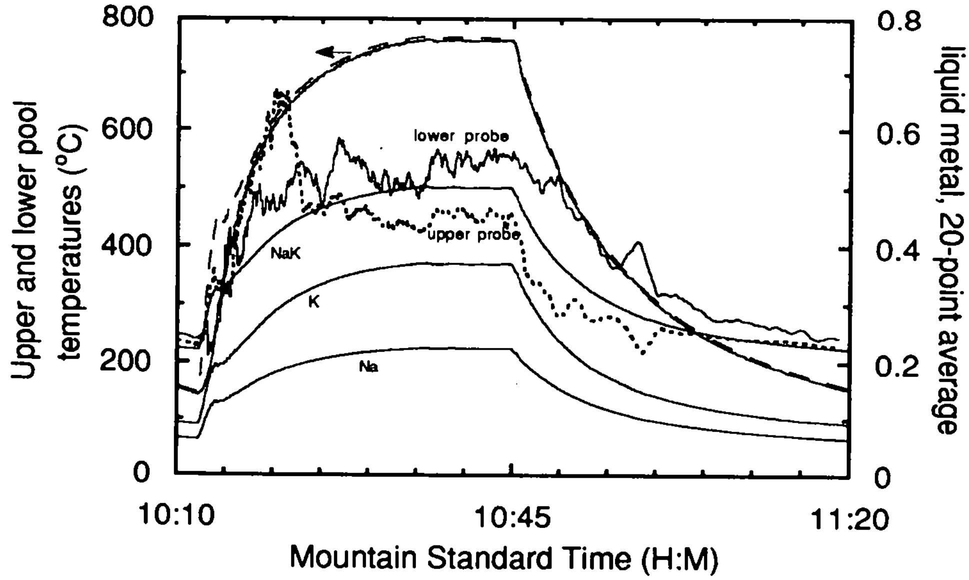

Figure 57. Measured temperature, and resistance measurements compared with model predictions for NaK-78 and for NaK-78 separated into its constituents.

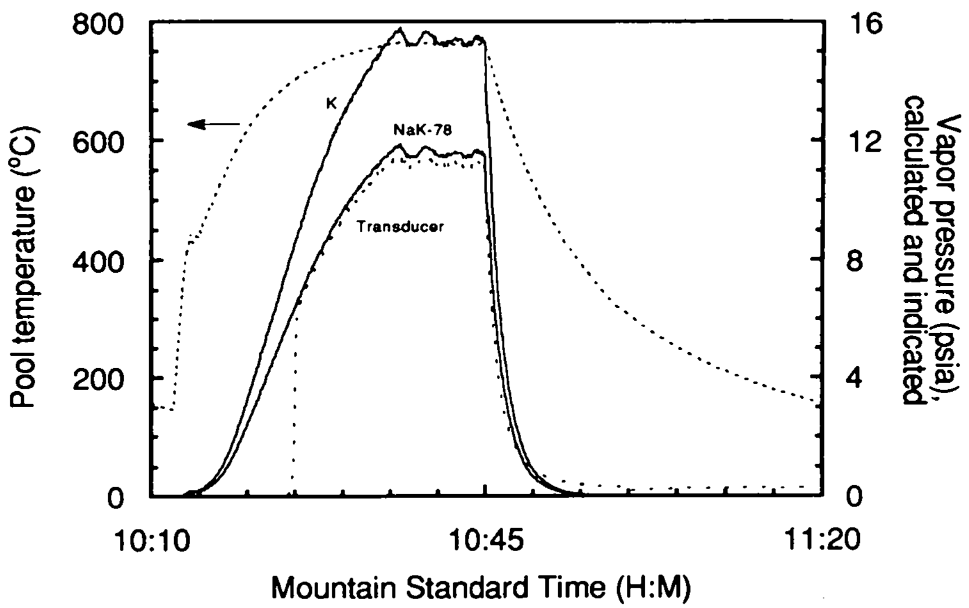

Figure 58. Calculated potassium and NaK-78 vapor pressures, the measured pool temperature used to calulate them, and measured pool pressure, during a boiling run.

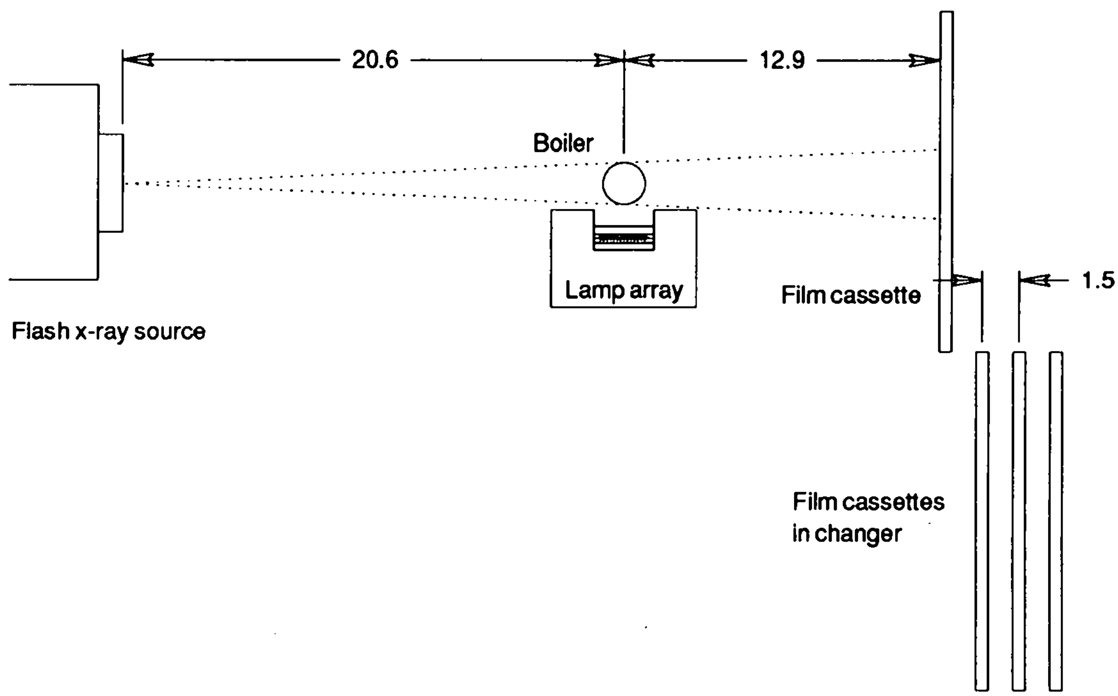

Figure 59. Flash radiography equipment layout and dimensions (top view).

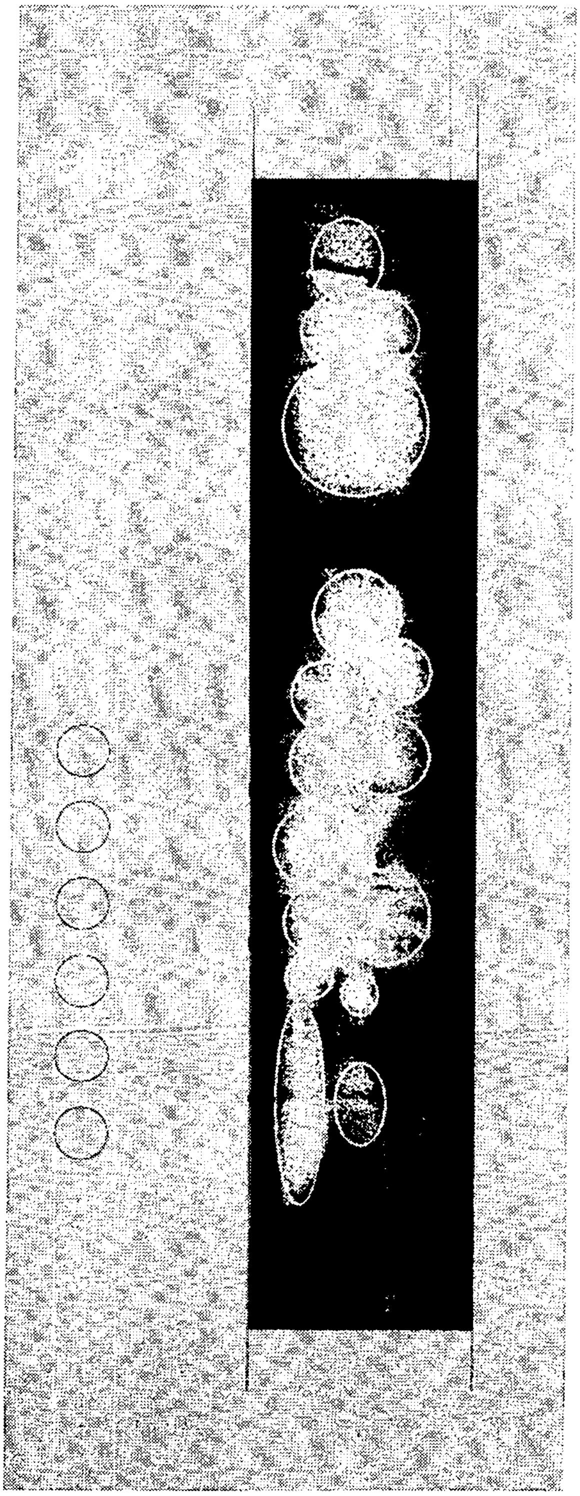

Figure 60. First X-ray image of bubbles in Thermacore-coated tube at 650°C. Lines show location of lamps and boiler sides. Lamps serve as scale: approximately 1-cm diameter.

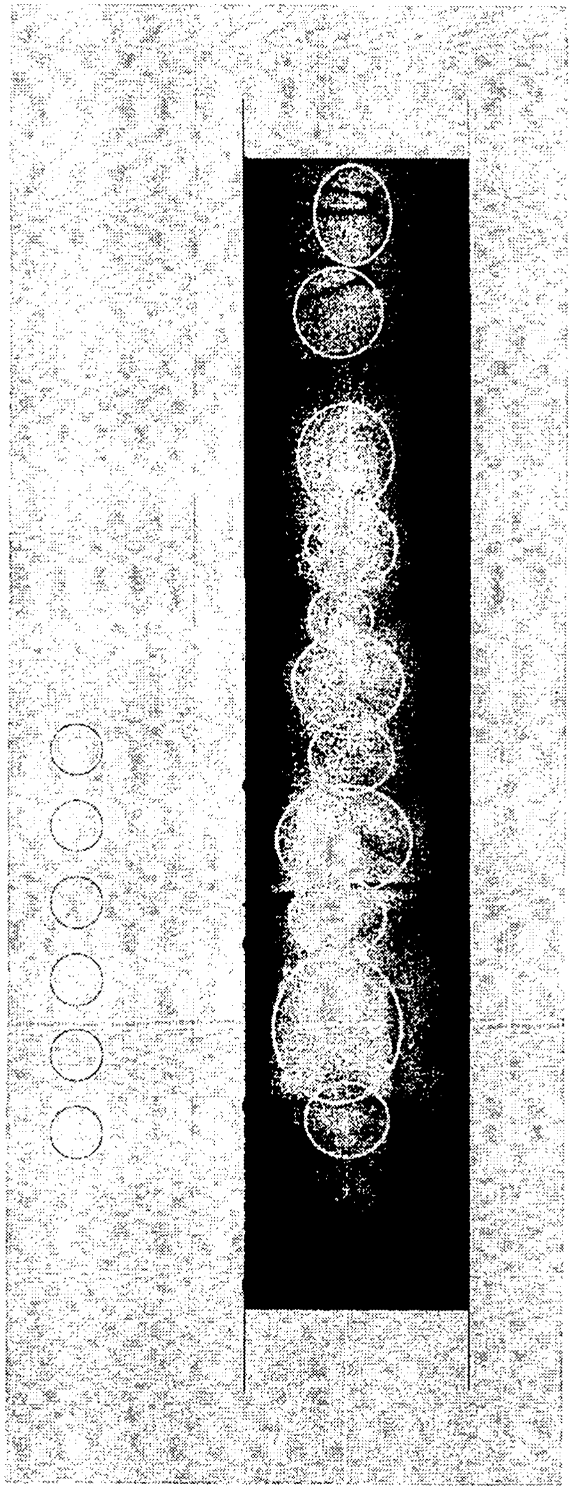

Figure 61. Second X-ray image of bubbles in Thermacore-coated tube at 650°C. Lines show location of lamps and boiler sides. Lamps serve as scale: approximately 1-cm diameter.

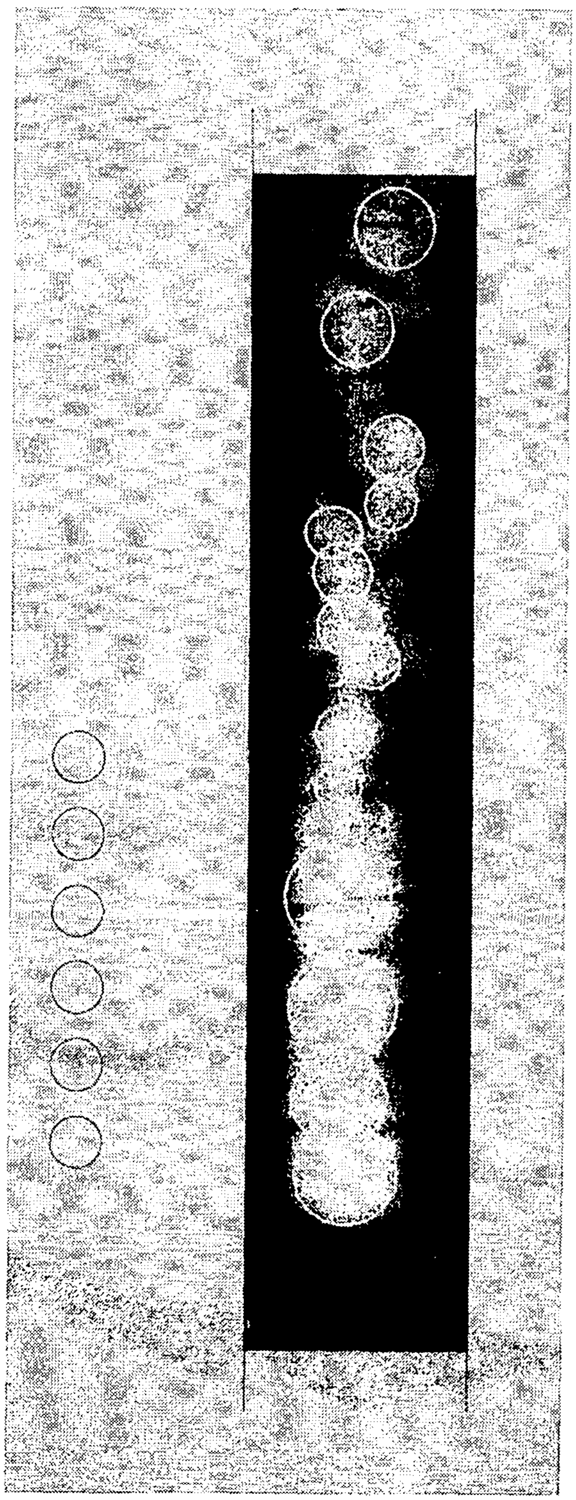

Figure 62. First X-ray image of bubbles in Thermacore-coated tube at 700°C. Lines show location of lamps and boiler sides. Lamps serve as scale: approximately 1-cm diameter.

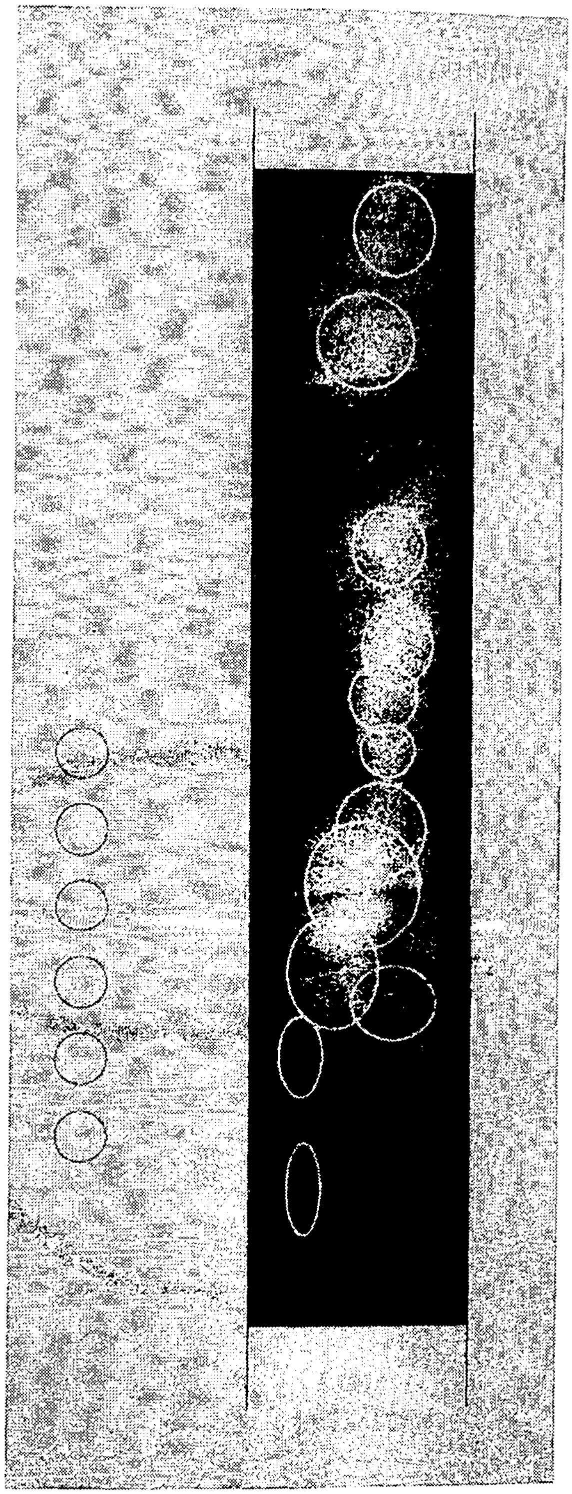

Figure 63. Second X-ray image of bubbles in Thermacore-coated tube at 700°C. Lines show location of lamps and boiler sides. Lamps serve as scale: approximately 1-cm diameter.

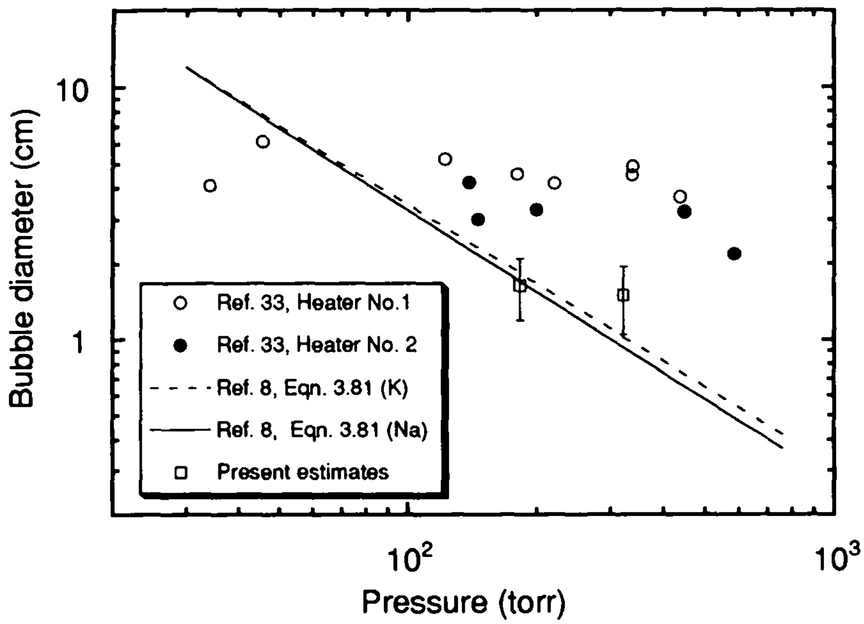

Figure 64. Comparison of bubble sizes in NaK-78 (present), potassium [36], and the correlation of Rohsenow and Cole [37].

Distribution:

U.S. Department of Energy (5)
Forrestal Building
Code CE-132
1000 Independence Avenue, SW
Washington, DC 20585
Attn: G. Burch
S. Gronich

U.S. Department of Energy (2)
Forrestal Building
Code CE-13
1000 Independence Avenue, SW
Washington, DC 20585
Attn: R. Annan

U.S. Department of Energy (2)
Albuquerque Operations Office
P.O. Box 5400
Albuquerque, NM 87115
Attn: G. Tennyson
N. Lackey

U.S. Department of Energy
San Francisco Operations Office
1333 Broadway
Oakland, CA 94612
Attn: R. Hughey

Arizona Solar Energy Office
Dept. of Commerce
1700 W. Washington, 5th Floor
Phoenix, AZ 85007
Attn: F. Mancini

Australian National University
Department of Engineering Physics
P. O. Box 4
Canberra ACT 2600 AUSTRALIA
Attn: S. Kaneff

Battelle Pacific Northwest Laboratory
P.O. Box 999
Richland, WA 99352
Attn: D. Brown

California Polytechnic University
Dept. of Mechanical Engineering
3801 West Temple Avenue Engineering
Pomona, CA 91768
Attn: W. Stine

Clever Fellows
Innovation Consortium, Inc.
R.D. 1, Box 410, River Road
Melrose, NY 12121
Attn: J. A. Corey, P.E.

Cummins Power Generation (2)
MC 60125
P. O. Box 3005
Columbus, IN 47202-3005
Attn: R. Kubo

Cummins Power Generation South
150 Tannehill Drive
Abilene, TX 79602
Attn: M. McGlaun

DLR
Pfaffenwaldring 38-40
7000 Stuttgart 80 GERMANY
Attn: R. Buck

Dynatherm Corporation
1 Beaver Court
P.O. Box 398
Cockeysville, MD 21030
Attn: David Wolf

Electric Power Research Institute
P.O. Box 10412
Palo Alto, CA 94303
Attn: J. Schaeffer

Energy Research Centre
R. S. Phy. Sc.
Australian National University
Canberra ACT 2601 AUSTRIALIA
Attn: K. Inall

Energy Technology Engr. Center (2)
Rockwell International Corp.
P. O. Box 1449
Canoga Park, CA 91304
Attn: W. Bigelow
R. LeChevalier

Florida Solar Energy Center
300 State Road, Suite 401
Cape Canaveral, FL 32920
Attn: Library

Georgia Power
7 Solar Circle
Shenandoah, GA 30265
Attn: W. King

Institute of Gas Technology
34245 State Street
Chicago, IL 60616
Attn: Library

Jet Propulsion Laboratory
4800 Oak Grove Drive
Pasadena, CA 91109
Attn: M. Alper

Lawrence Berkeley Laboratory
MS 90-2024
One Cyclotron Road
Berkeley, CA 94720
Attn: A. Hunt

Los Alamos National Laboratory
MEE13
Los Alamos, NM 87545
Attn: M. Merrigan

McDonnell-Douglas Astronautics Company
5301 Bolsa Avenue
Huntington Beach, CA 92647
Attn: R. L. Gervais,
J. Rogan,
D. Steinmeyer

Mechanical Technology, Inc. (2)
968 Albany Shaker Road
Latham, NY 12110
Attn: G. Dochat
J. Wagner

NASA Lewis Research Center (4)
21000 Brook Park Road
Cleveland, OH 44135
Attn: R. Shaltens
J. Schrieber

National Renewable Energy
Laboratory (6)
1617 Cole Boulevard
Golden, CO 80401
Attn: T. Williams
L. M. Murphy
G. Jorgensen
T. Wendelin
A. Lewandowski
M. Bohn

Northern Research and Engineering Corp.
39 Olympia Avenue
Woburn, MA 01801-2073
Attn: J. Kesseli

Power Kinetics, Inc.
415 River Street
Troy, NY 12180-2822
Attn: W. E. Rogers

Research International
18706 142nd Avenue NE
Woodinville, WA 98072
Attn: E. Saaski

Schlaich, Bergermann & Partner
Hohenzollernstr. 1
D - 7000 Stuttgart 1 GERMANY
Attn: W. Schiel

Science Applications International
Corporation
10343 Roselle Street, Suite G
San Diego, CA 92121
Attn: K. Beninga

Science Applications International
Corporation
Mail Stop 32
10260 Campus Point Court
San Diego, CA 92121
Attn: B. Butler

Solar Energy Industries Assoc. (2)
777 North Capitol St. NE
Suite 805
Washington, D.C. 20002
Attn: S. Sklar
K. Sheinkopf

Solar Kinetics, Inc. (2)
P.O. Box 540636
Dallas, TX 75354-0636
Attn: J. A. Hutchison
P. Schertz

Stirling Technology Company (3)
2952 George Washington Way
Richland, WA 99352
Attn: Mr. Maurice A. White

Stirling Thermal Motors (2)
2841 Boardwalk
Ann Arbor, MI 48104
Attn: Lennart Johansson

Stirling Machine World
1823 Hummingbird Court
West Richland, WA 99352-9542
Attn: Brad Ross

Sunpower, Inc.
6 Byard Street
Athens, OH 45701
Attn: W. Beale

Thermacore, Inc. (2)
780 Eden Road
Lancaster, PA 17601
Attn: Mr. Donald Ernst

University of Houston
Solar Energy Laboratory
4800 Calhoun
Houston, TX 77704
Attn: J. Richardson

University of Minnesota
Dept. of Mechanical Engineering
111 Church St., SE
Minneapolis, MN 55455
Attn: E. A. Fletcher

Sandia Internal Distribution:

1513	D. R. Adkins
1513	R. C. Dykhuizen
1513	R. D. Skocypec
6000	D. L. Hartley
6200	D. E. Arvizu
6201	P. C. Klimas
6215	C. P. Cameron
6215	P. G. Cordeiro
6215	K. S. Rawlinson
6216	C. E. Tyner
6216	C. E. Andraka
6216	R. B. Diver
6216	T. R. Mancini
6216	D. F. Menicucci
6216	J. B. Moreno (5)
6216	T. A. Moss(5)
7141	Technical Library (5)
7151	Technical Publications
7613-2	Document Processing for DOE/OSTI (10)
8523-2	Central Technical Files

THIS PAGE INTENTIONALLY LEFT BLANK